The University of Alberta
Printing Department
Edmonton, Alberta

THE UNIVERSITY OF ALBERTA

SHALLOW SHELLS SUPPORTED BY ELASTIC BEAMS

by

© DAVID HAROLD QUAPP

A THESIS

SUBMITTED TO THE FACULTY OF GRADUATE STUDIES

IN PARTIAL FULFILMENT OF THE REQUIREMENTS FOR THE DEGREE

OF MASTER OF SCIENCE

DEPARTMENT OF CIVIL ENGINEERING

EDMONTON, ALBERTA

SPRING, 1969

UNIVERSITY OF ALBERTA

FACULTY OF GRADUATE STUDIES

The undersigned certify that they have read, and recommend to the Faculty of Graduate Studies for acceptance, a thesis entitled SHALLOW SHELLS SUPPORTED BY ELASTIC BEAMS submitted by David Harold Quapp in partial fulfilment of the requirements for the degree of Master of Science.

ABSTRACT

A numerical analysis, which takes into account the effects of bending, is used to determine the effects on shallow elliptic paraboloid shells of various boundary conditions, including elastic edge beams. A computer program was written to solve the simultaneous linear equilibrium equations resulting from the analogue. The shells studied are square in planform, and normal uniform loadings are considered. Boundary conditions are handled by assigning values to stiffness parameters defined corresponding to displacements in each of the three co-ordinate directions and to rotation about an axis along the edge.

The effects of idealized boundary conditions on stress resultants and deflections of the shell are presented. It is shown that the idealized boundary conditions yield results differing significantly from the results of elastic edge beams of practical shapes and sizes. Interactions of the shell surface and the supporting edge members are discussed. The study treats briefly the effects of varying curvature of a shell with elastic edge beams of practical size.

ACKNOWLEDGMENTS

The author is extremely grateful to Dr. S. H. Simmonds, Associate Professor of Civil Engineering, for generously providing guidance and encouragement in the preparation of this thesis.

Financial assistance was arranged through the Government of the Province of Alberta by Mr. E. J. Sanden, Chief Bridge Engineer of the Department of Highways, and is hereby gratefully acknowledged.

A note of thanks is due to draughtsman Mr. Mark Filipiak, and to Mrs. Gail Mitchinson for typing the manuscript.

It is also a pleasure to acknowledge the untiring support given by the author's wife, Mary.

LIST OF TABLES

LIST OF FIGURES

NOMENCLATURE

a,b	= shell dimensions, semi-spans in the x and y dimensions, respectively.
h_x, h_y, h	= shell dimensions, semi-spans in the x and y directions, respectively. For symmetrical shells, $h = h_x = h_y$.
K1, K2, K3, K4	= edge beam stiffness parameters which relate the beam's axial stiffness, transverse bending stiffness, torsional stiffness, and in-plane bending stiffness, respectively, to the axial stiffness and transverse bending stiffness of the shell over a grid-length.
Mxx, Nyy	= bending moments in the shell acting over a grid-length.
Mxy	= twisting moments in the shell acting over a grid-length.
Nxx, Nyy	= membrane direct stress resultants in the shell acting over a grid-length.
Nxy	= membrane shear stress resultants in the shell acting over a grid-length.
t	= thickness of the shell.
u, v, w	= displacement components in the tangential x, tangential y, and normal z directions, respectively.
x, y, z	= Cartesian co-ordinates of the reference system.

CHAPTER I

INTRODUCTION

In the design of translational shells the designer is faced with the problem of selecting edge members which are compatible with his analysis. Generally, the assumptions used in the analysis for the deformation characteristics of the supports are unrealistic and, at present, there is little in the literature to guide him in choosing the optimum area and shape of cross-section which will minimize the stresses in the shell. It is the solution of this problem which forms the purpose of this investigation.

The design of translational shells has been based generally on stress resultants obtained from a membrane analysis. This analysis is known to give satisfactory results for uniformly distributed loads over the shell surface in regions sufficiently remote from the edge supports. However, the membrane analysis assumes that only in-plane shear stresses are transferred to the edge members and that the edge member has negligible stiffness in all directions except in the axial direction which is considered rigid, assumptions of questionable validity.

More general theories for the analysis of translational shells have been presented (2) (9)*. These theories formulate the governing differential equation for the shell surface taking into account both membrane and bending stress resultants.

---

* Numbers in brackets ( ) refer to list of references.

Unfortunately, a general solution of these equations is not possible and solutions for only a few idealized boundary conditions have been obtained by using numerical techniques (3) (1).

More recently mathematical analogues or models have been developed which permit simulation of the deformation characteristics of both the shell surface and the supporting edge members (5) (6). Thus this technique makes possible the study of actual edge members having finite dimensions and finite stiffnesses, rather than idealized boundaries. From such a study the designer may obtain some insight into the interaction of the shell surface and the supporting edge members. The effects of varying the area and shape of rectangular cross-sections of edge members on the magnitudes and distributions of the stress resultants in the shell forms the major portion of this thesis.

The results presented were obtained for elliptic paraboloid shells using the analogue developed by Rajendram (5). A brief description of this analogue and the computer program used is given in Chapter II.

Chapter III contains a discussion of the variables considered. Four stiffness parameters were defined corresponding to displacements in each of the three co-ordinate directions and to a rotation about an axis along the edge. To evaluate qualitatively the effects of each stiffness parameter on the behaviour of the shell, the parameters were assigned values of zero and infinity in all possible combinations. The results from this series are presented in Chapter IV.

The stiffness parameters were then evaluated for a series of finite edge members of square cross-section where the dimensions were varied to determine the effect of changing the cross-sectional area and for another series where the cross-sectional area was kept constant but the ratio of the dimensions was varied to determine the effect of shape. In a third series, the rise of the shell was varied to determine the effect of curvature. These results with edge members having finite dimensions are presented in Chapter V.

A summary of the major conclusions is given in Chapter VI.

CHAPTER II

METHOD OF ANALYSIS

2.1 Description and Application of the Analogue

An analogue consisting of rigid bars connecting deformable elastic hinges was developed by Rajendram (5) to simulate the action of shallow doubly-curved translational shells. A rectangular grid of primary bars resists bending and in-plane direct stresses while a secondary grid intersecting the primary grid at the grid midpoints resists the in-plane membrane shear stresses. Changes in curvature and in-plane extensions are considered to be concentrated at the grid intersection points. Since compatibility of geometry is assured with the analogue only equations of equilibrium are required. These yield results for the shell surface which are identical to those obtained by finite difference operators applied to the governing differential equation for these shells. In a similar manner modifications can be made to the analogue at the boundaries to simulate the presence of elastic edge members. The equations of equilibrium for gridpoints near their location will include in addition to the shell parameter the edge beam stiffness parameters K1, K2, K3 and K4, which relate the beam's axial stiffness, transverse bending stiffness, torsional stiffness, and in-plane bending stiffness, respectively, to the stiffness of the shell over a grid-length.

These equilibrium equations result in a set of linear, algebraic, simultaneous equations in terms of the unknown midsurface displacements, from which, by means of the established relationships, the stress resultants in the shell are calculated.

2.2 Basic Assumptions of the Analogue

The analogue is restricted to doubly curved shells of translation, of rectangular planform, in which the middle surface of the shell is represented in Cartesian co-ordinates by the equation

$$z = h_x \, x^2/a^2 + h_y \, y^2/b^2$$

The assumptions on which the analogue is based are given below:

(i) The limitations of the theory of elasticity apply.

(ii) The shell is shallow. This leads to the result that the curvatures of the shell in the x and y directions are constants, $2h_x/a^2$ and $2h_y/b^2$, respectively. In addition, the distance between any two points, in the middle surface of the shell, is approximately equal to the projected length in the horizontal plane.

(iii) The effects of the normal shears on the equilibrium equations are negligible.

(iv) The effects of the displacements in the tangential directions

on the changes in curvature and twist are considered negligible compared to the effect from the normal displacements.

(v) The thickness of the shell is small compared to the radius of curvature of the shell, and the displacements are small compared to the thickness of the shell.

(vi) The loadings on the shell are concentrated at the primary and secondary grid points, and act in the normal and tangential directions.

(vii) The force effects that act over a grid length are concentrated at the primary and secondary grid points.

(viii) The centroids of the edge beams are concentrated along the edge of the shell at the middle surface.

2.3 Computer Program for Solving the Analogue

A computer program was written to generate and solve the large number of equilibrium equations that are required to adequately describe the behaviour of the shell. The large matrix, having a sparse population of non-zero elements, was solved by the Gauss elimination method, using a diagonal subscripting method (10) for reasons of computing efficiency.

Within the restriction of requiring two-fold symmetry in the shell, this program will solve a variety of structures, although, for the purpose of this study, a specific shell with limited edge

beam configurations was solved. Thus, besides the elliptic paraboloid considered, such shells as parabolic cylinders, hyperbolic paraboloids, and paraboloids of revolution can be handled, as well as plates, all with elastic edge members. A further feature of the program is that the edge beam stiffnesses can be varied over the length of the members. Provision was made so that up to six loading conditions can be applied to the shell in one computing run.

The imput to the program consists of the number of grid lengths in the x and y directions; the shell dimensions a, b, h_x, h_y and t; the material properties of the shell; the imposed movements of the corners of the shell; the values of the edge beam stiffnesses; and a code for identifying the loading cases to be considered.

Besides a listing of the input data, the computer output consists of displacements, and the stress resultants from the shearing forces, direct forces, bending moments and twisting moments, in the x and y directions, at the primary and secondary grid points.

Since the shells reported are square they have four-fold symmetry, but the program handled the calculations on the basis of two-fold symmetry, thus an indication of the accuracy in the simultaneous solution of the equilibrium equations would be apparent by comparing the symmetry of the calculated results. A 10 by 10 square grid, resulting in 382 simultaneous equations, was used throughout and from which excellent symmetry was observed in all cases.

Using an IBM 7040 computer, approximately 18 minutes is required for solving one shell. This is reduced to 1.5 minutes with the more powerful IBM 360 MOD/67 computer.

Additional refinements to the program, for extending its usefulness, can readily be made.

2.4 Comparison of Analogue with Existing Results

The membrane analysis (4) assumes that only in-plane shear stresses are transferred to the edge member, and that the edge beam has stiffness only in the axial direction, which is considered rigid. Comparisons of the results obtained from the analogue are made with those from the membrane solution in CHAPTERS IV and V, from which it appears that in areas well away from the edge, the direct stress resultants and the shearing stress resultants agree exactly between the two methods.

To obtain some indication of the accuracy obtained from the analogue, results were compared with those given by Abu-Sitta (1) and in general there is excellent agreement. A discussion of the comparison is given elsewhere by Simmonds (7). Some of the differences that appear near the edge can possibly be accounted for by the difference in the method of defining the edge beam displacements.

If the radius of curvature of the shell is made very large, the analogue will approximate a plate. To obtain some further indication of the accuracy of the results obtained from the analogue,

three plates were analyzed, one plate having clamped edges, one having simply supported edges, and another with supports at the corner only. The results were compared with plate theory (8), for center deflection, moment at the center, and moment at the mid-edge for the last case. Exact agreement existed for the simply supported case, and a maximum difference of 1.7% occurred for the clamped edge case. The largest difference occurred for the plate supported at the corners, in which the analogue gave a mid-edge moment that was 7% below that of the classical method, and differences of 2.5% or less for deflection and moment at the center.

2.5 Summary

It would appear that the solution of the analogue, using the computer program developed, yields results that compare favourably with those presented elsewhere.

CHAPTER III

VARIABLES CONSIDERED IN THE ANALYSIS

3.1 Introductory Remarks

This chapter describes the shell and its supporting edge member, and gives the reasons for the choice and range of the parameters used in the study. Of the four series presented, three involve edge beam configurations, and one involves the rise to span ratio of the shell.

3.2 Description of the Shell and the Supporting Edge Beams

Considerations are limited to elliptic paraboloid shells. The dimensions used were chosen to enable comparison to be made with the published results of Abu-Sitta (1).

As shown in FIGURE 3.1(a), the shell is square in planform, and is symmetrical about both crowns, which are coincident with the co-ordinate axes. The lengths of both edges are $2a = 2b = 8$ ft.; rises $h = h_x = h_y$ at the edge are 0.64 ft., and the thickness t is 0.03575 ft. The modulus of elasticity was set at 700,000 ksf, and Poisson's ratio was zero. The preceding shell configuration is referred to as the "standard shell" in the discussions that follow.

FIGURE 3.1(b) shows the supporting edge beam, which has its axes normal and tangent to the shell. For calculating the stiffnesses K1, K2, K3 and K4 the physical dimensions of the edge beam were used, except for one series in which the stiffnesses were assigned zero or

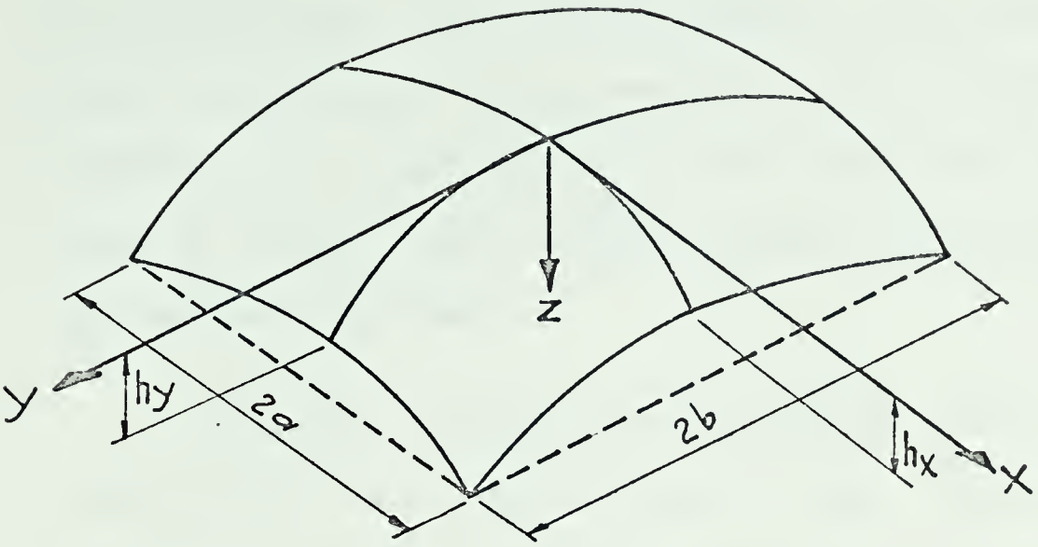

a) Elliptic Paraboloid Shell

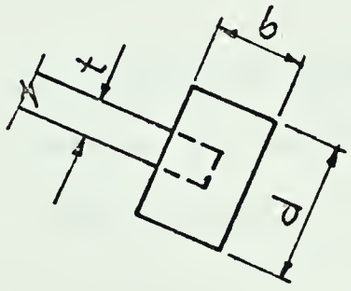

b) Edge Member

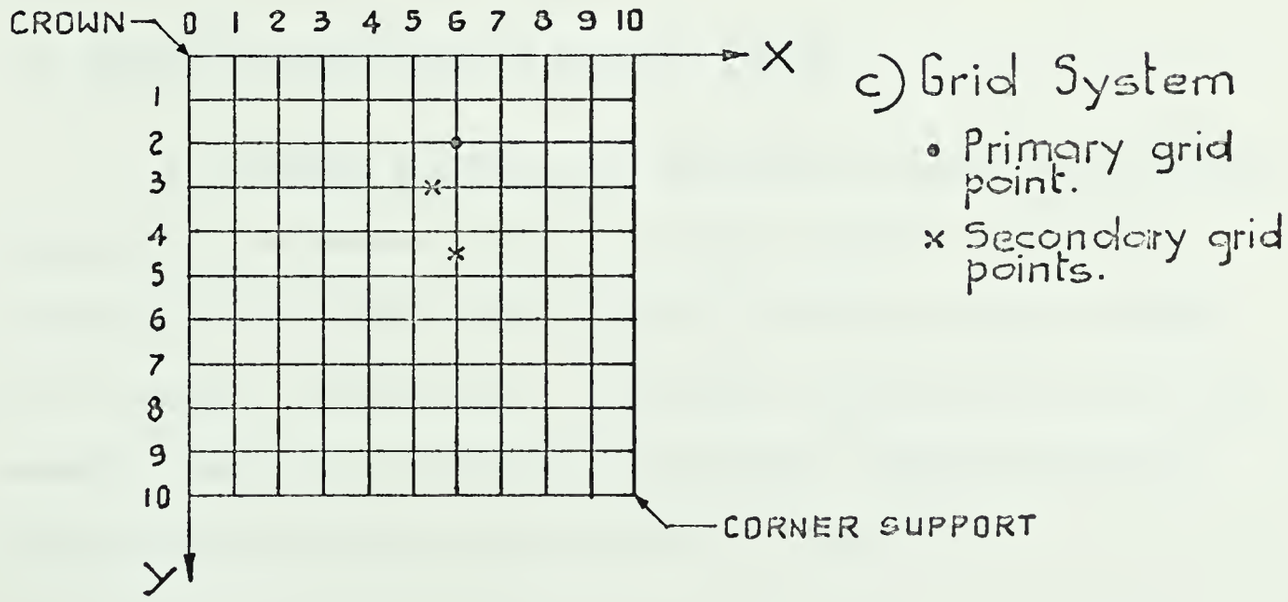

c) Grid System

- Primary grid point.
- × Secondary grid points.

FIGURE 3.1 THE ELLIPTIC PARABOLOID SHELL

very large values. The numerical values of the stiffnesses are given in TABLE 3.1. A square edge beam, with cross-sectional dimensions of 4t, was selected to permit comparisons to be made among the series. This edge beam configuration is referred to as the "standard edge beam".

A uniform loading of 100 psf, applied normal to the surface of the shell, was used for all cases. The corner supports were constrained against movement, although the analysis and the computer program will handle such movements.

To facilitate positional description on the shell's surface, reference is made to primary and secondary grid points which relate to intersections and mid-points between intersections of the square grid system, as shown in FIGURE 3.1(c). Thus x = 0.8a refers to a primary grid-line and x = 0.85a refers to a secondary grid-line.

3.3 Parameters for Idealized Boundary Series

To evaluate qualitatively the effects of each edge stiffness parameter on the behaviour of the "standard shell", the four stiffnesses were assigned the limiting values of zero and infinity in all possible combinations. The sixteen combinations include those boundary conditions commonly known as roller, hinged or built-in. Results from this series are presented in Chapter IV.

TABLE 3.1

VALUES OF ELASTIC EDGE BEAM STIFFNESS PARAMETERS

SIZE OF EDGE BEAM SERIES

d = b	K1	K3	K2 = K4
0t	0	0	0
2t	0.35	1.26	1.43
* 4t	1.43	19.3	22.9
6t	3.22	97.7	116.
8t	5.72	308.	366.
10t	8.94	754.	894.
100t	894.	$754. \times 10^4$	$894. \times 10^4$
1000t	$894. \times 10^2$	$754. \times 10^8$	$894. \times 10^8$

SHAPE OF EDGE BEAM SERIES

d:b	d	b	K1	K2	K3	K4
1000:1	126.t	.013t	1.43	22,900	0.05	0.02
3:1	6.9 t	2.3 t	"	68.6	12.0	7.63
2:1	5.7 t	2.8 t	"	45.8	15.7	11.4
* 1:1	4.0 t	4.0 t	"	22.9	19.3	22.9
1:2	2.8 t	5.7 t	"	11.4	15.7	45.8
1:3	2.3 t	6.9 t	"	7.63	12.0	68.6
1:1000	.013t	126.t	"	0.02	0.05	22,900

* "Standard shell" with "Standard edge beam".

3.4 Parameters for Size of Edge Beam Series

This series was chosen to allow qualitative evaluation of the effects, on the "standard shell", of varying the cross-sectional area of square edge beams.

The beam dimensions varied from 0t, (effectively a free edge), through 2t, 4t, 6t, 8t, 10t and 100t, to 1000t (effectively a built-in edge). Most of the discussion centres on the practical range of edge beam sizes, from 4t to 10t.

TABLE 3.1 gives the numerical values of the stiffness parameters for square edge members. It is noted that the bending stiffnesses, K2 and K4, which are equal, increase much more rapidly than the axial stiffness parameter K1. The torsional stiffness parameter K3 is considered as a constant value of 0.8436K2. Therefore this series is a study mainly of the effects of K1 for small edge beams, and of the other stiffnesses for large edge beams. Results of this series are included in CHAPTER V.

3.5 Parameters for Shape of Edge Beam Series

To obtain further qualitative insight into the effects of boundary conditions, on the "standard shell", the shape of rectangular edge beams was varied in this series. The cross-sectional area was held at $16t^2$, equal to that of the "standard edge beam". The shape factor is presented by the depth to width ratio (d:b). It was assigned ratios of 3:1, 2:1, 1:1 ("standard edge beam"), 1:2, and 1:3. In addition, ratios of 1000:1 and 1:1000 are included to allow

comparison to be made with the idealized boundary series. Numerical values of the stiffness parameters appear in TABLE 3.1. Because the beam's cross-sectional area is constant, this series is a study mainly of the effects of varying the bending, and to a lesser extent, the torsional stiffnesses. Results are given in CHAPTER V.

3.6 Rise to Span Ratio Series

In order to generalize the results of the shape and size of edge beam series, the height $h_x = h_y$ of the shell was varied in this series. The standard edge member was used throughout. Results, which are presented in CHAPTER V, are discussed in terms of the ratio h/a (actually, rise to half-span ratio). Essentially this series deals with the effect of curvature on the shell.

3.7 Method of Presentation of Results

Chapters IV and V present the numerical results of the analyses. These consist of normal deflections, shearing forces Nxy, direct forces Nxx, bending moments Mxx and twisting moments Mxy, and are given for various locations in the shell. Results are shown for a quarter of the shell only, in the form of plots, tables and qualitative sketches. Because of symmetry, the effects in the y co-ordinate direction are a mirror image of the effects in the x direction, and will generally not be discussed, eliminating references to Nyy, Myy, Nyx and Myx. The membrane solution is included for reference purposes.

Considering sign conventions, deflections are positive downwards, positive moments cause compression at the top surface, and direct forces are positive in tension. Shearing stresses Nxy are positive when they form clockwise couples on elements of the shell viewed from below. The twisting moments Mxy are positive, using the right-hand rule, when the vector indicates tension on the face of the element.

CHAPTER IV

SHELLS WITH IDEALIZED BOUNDARY CONDITIONS

4.1 Introduction

To evaluate qualitatively the effects of each edge beam stiffness parameter on the behaviour of the shell, the parameters were assigned values of zero or infinity, in all possible combinations. Each of the sixteen combinations is identified by a letter, for example, Cases A, B, C, etc. To aid in the evaluation, the two combinations resulting from varying a particular stiffness parameter but keeping the others constant are paired in TABLE 4.1. For example, under the heading of Axial Stiffness K1, the first row shows that the stiffness parameter K1 is infinite for Case A and zero for Case D, while the remaining three stiffnesses are infinite. By using this table in conjunction with the graphical results appearing in the remainder of the chapter, the qualitative effects of varying any single parameter is quickly determined.

Only sixteen combinations of edge beam stiffnesses can occur, and some of these compare directly with the classical boundary conditions that permit ready analysis. Included in these are the roller support (Case B); the hinged support (Case C); the unrestrained, or free, edge (Case Q); the fixed, or built-in, edge

TABLE 4.1

VALUES OF EDGE BEAM STIFFNESS PARAMETERS

FOR IDEALIZED BOUNDARY SERIES

Axial Stiffness K1					Transverse Bend. Stiff. K2				
Cases	K1	K2	K3	K4	Cases	K1	K2	K3	K4
A,D	1,0	1	1	1	A,H	1	1,0	1	1
C,F	1,0	1	0	1	C,M	1	1,0	0	1
H,I	1,0	0	1	1	D,I	0	1,0	1	1
M,K	1,0	0	0	1	K,F	0	1,0	0	1
J,F	1,0	1	1	0	J,P	1	1,0	1	0
B,E	1,0	1	0	0	B,N	1	1,0	0	0
P,L	1,0	0	1	0	G,L	0	1,0	1	0
N,Q	1,0	0	0	0	E,Q	0	1,0	0	0

Torsional Stiffness K3					In-plane Bending Stiff.K4				
Cases	K1	K2	K3	K4	Cases	K1	K2	K3	K4
A,C	1	1	1,0	1	A,H	1	1	1	1,0
H,M	1	0	1,0	1	C,B	1	1	0	1,0
D,F	0	1	1,0	1	H,P	1	0	1	1,0
I,K	0	0	1,0	1	M,N	1	0	0	1,0
J,B	1	1	1,0	0	D,G	0	1	1	1,0
P,N	1	0	1,0	0	F,E	0	1	0	1,0
G,E	0	1	1,0	0	I,L	0	0	1	1,0
L,Q	0	0	1,0	0	K,Q	0	0	0	1,0

Note: 1 = infinite stiffness; 0 = zero stiffness

(Case A); and the continuous edge (Case I). It is to be noted that the usual definitions for hinged and roller supports, as used in strength of materials, relate to simpler structural systems which do not involve the constraint represented by the axial stiffness parameter K1.

4.2 Normal Deflections

Considering all the possible combinations of zero or infinity for the four stiffness parameters K1, K2, K3 and K4, four distinct groups are evident according to the magnitudes of the deflections encountered. In TABLE 4.2, which gives the magnitudes of the normal deflections at the crown, at the mid-edge, and of the maximum deflection, the four groups are separated from each other by solid lines. The deflections along the crown line of the shell (the line extending from the crown to the edge along one of the co-ordinate axes) are given in FIGURE 4.1. For comparison, the deflections for the shell with the standard edge member are also given on the same figure.

The deflections for each case of the first group (Cases I, K, F, M, D, H, A, and C) are close in magnitude to those of the shell with built-in boundaries, Case A. In all of these cases the stiffness K4 is infinite. It would appear that in each of these cases the shell is supported at the edge primarily by in-plane direct forces, and only small variations in deflection exist due

TABLE 4.2

NORMAL DEFLECTIONS FOR IDEALIZED BOUNDARY SERIES

Case	Edge Beam Stiffnesses *				Crown Deflection	Mid-edge Deflection	Maximum Deflection	
	K1	K2	K3	K4	x 10,000	x 10,000	x 10,000	Location
I	0	0	1	1	.785a	.694a	.740a	Note 1
K	0	0	0	1	.784a	.784a	.804a	"
F	0	1	0	1	.841a	0	.915a	"
M	1	0	0	1	.832a	0	.925a	"
D	0	1	1	1	.874a	0	.927a	"
H	1	0	1	1	.834a	0	.935a	"
A	1	1	1	1	.861a	0	.937a	"
C	1	1	0	1	.831a	0	.941a	"
J	1	1	1	0	1.56a	0	1.65a	Note 1
P	1	0	1	0	1.56a	0	1.65a	"
B	1	1	0	0	1.56a	0	1.70a	"
N	1	0	0	0	1.56a	0	1.70a	"
G	0	1	1	0	3.32a	0	3.69a	Note 2
E	0	1	0	0	3.67a	0	4.37a	"
L	0	0	1	0	10.6a	25.2a	25.2a	Mid-edge
Q	0	0	0	0	13.3a	35.4a	35.4a	"

* 1 = infinite stiffness; 0 = zero stiffness.

Note 1: On diagonal, 0.3a from edge of the shell.

Note 2: On crown line, 0.3a from edge of the shell.

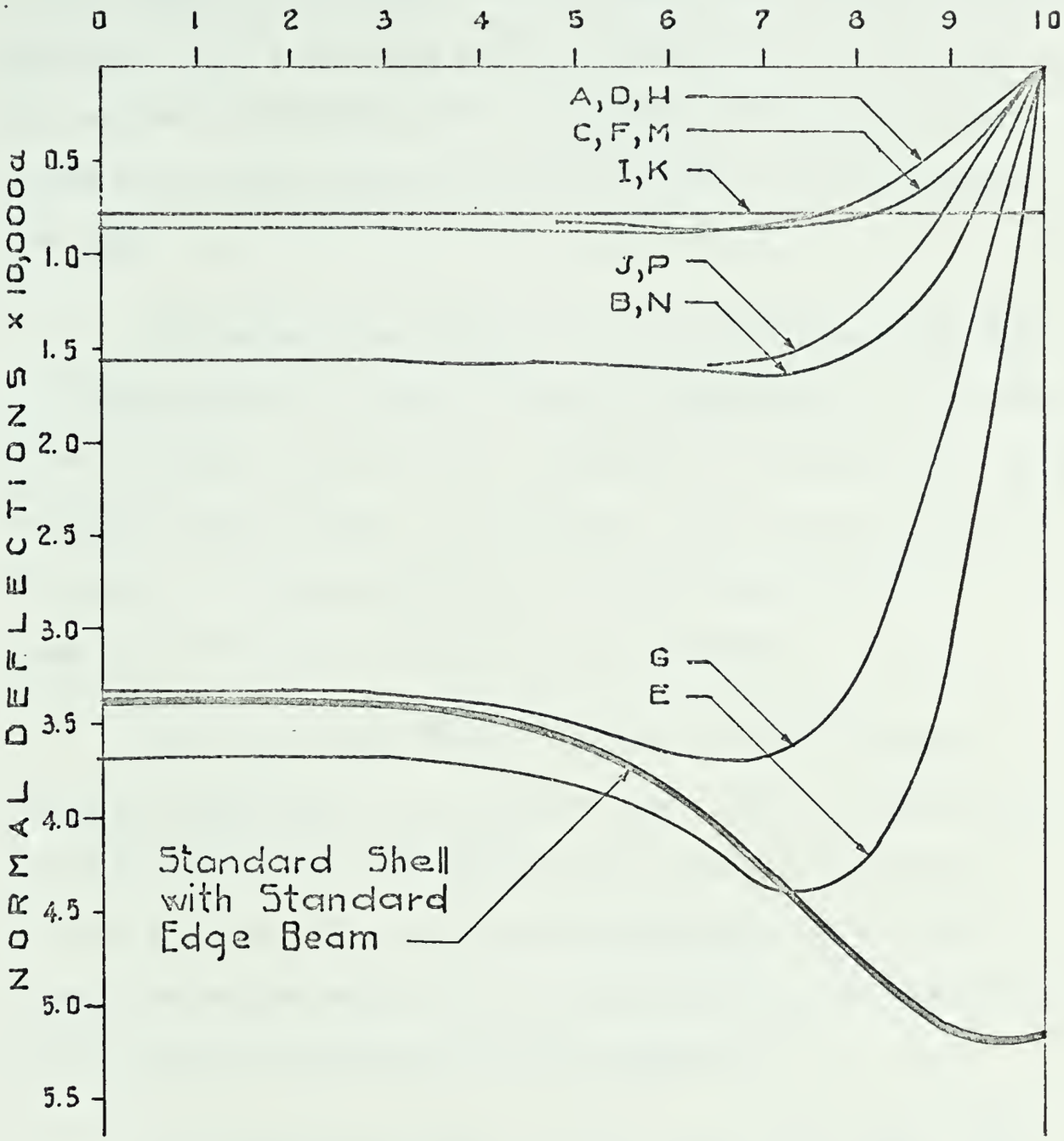

FIGURE 4.1 NORMAL DEFLECTIONS ALONG CROWN LINE FOR IDEALIZED BOUNDARY SERIES

to the effects of transverse forces (normal shear forces), in-plane shearing forces and bending moments, if they exist, at the edge. The smallest deflections of all the combinations occur for Cases I and K, for which only in-plane direct forces are acting along the edge.

The second group (Cases J, P, B, N) has deflections about 1.8 times greater than those of Case A. This group is characterized by K1 = infinity and the shell is supported at the edge primarily by in-plane shearing forces. Direct forces across the edge are zero. The effect of transverse forces or bending moments induced at the edge, on deflections in the shell, is very small.

The third group (Cases G, E) has deflections roughly 4 times the deflections of the built-in case. Here the edge of the shell is supported by transverse forces, ie K2 = infinity and K1 = K4 = 0. The effect on maximum deflection of eliminating transverse bending moments at the edge (Case E) is now much greater than it was for the previous groups considered.

The last group (Cases L, Q) has large deflections. For both cases, at the edge of the shell, the shearing forces, the transverse forces, and the direct forces across the edge are zero. If the shell is prevented from rotating at the edge (Case L), the crown deflection is 11 times greater than for the built-in shell, Case A. For a free edge (Case Q), the crown deflection is 16 times as great as for the built-in case.

In the twelve cases where the edge member can provide either a membrane shearing force or direct force along the edge, the maximum deflections are greater by not more than 13% of the crown deflections, and occur along the diagonal of the shell a distance of about 0.3a from the edges of the shell. However, when only transverse forces can be resisted (ie membrane reactions are zero), the maximum deflections occur along the crown line, at a point 0.3a from the edge, and are less than 19% greater than the crown deflections.

For free edges, the shell's deflection pattern is entirely different, with large downward deflections occurring at the mid-edge, and the shell rising near the supports.

4.3 Direct Stress Resultants Nxx

Again, as in the case of normal deflections, the direct stress patterns of the sixteen combinations can be distinctly grouped according to the edge beam stiffness parameter values. The Nxx patterns for these groups are shown in FIGURE 4.2 in the form of sketches, and TABLE 4.3 provides the maximum and minimum values.

Two major groups of Nxx patterns exist, for K4 = infinity (sketches a, b, c) and for K4 = 0 (sketches d, e, f). These are characterized by the existence, or non-existence, respectively, of direct stresses across the edge x = a. Variations in Nxx within each major group, reflecting the effects of the remaining stiffnesses,

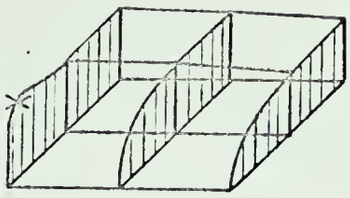

a) Cases A,H,C,M.

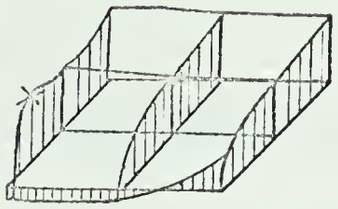

b) Cases D,F.

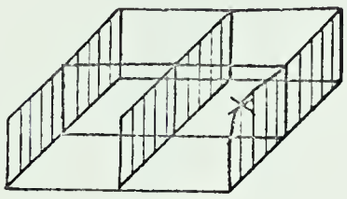

c) Cases K,I.

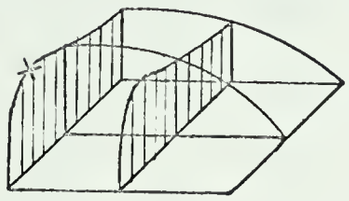

d) Cases N,J,P,B.

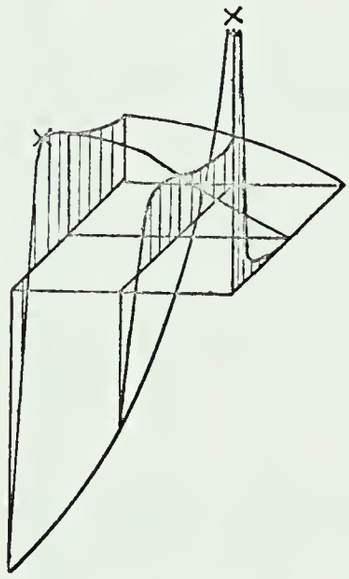

e) Cases E,G.

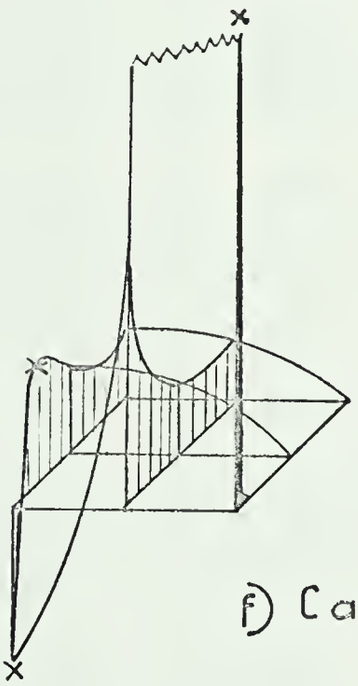

f) Cases Q,L.

Refer to TABLE 4.5 for maximum Nxx values at points marked "x". Sketches are to scale for first case in each list.

Scale: I = 500 Lbs/ft.

Axes :

FIGURE 4.2 DIRECT STRESS Nxx DISTRIBUTIONS FOR IDEALIZED BOUNDARY SERIES

TABLE 4.3

DIRECT STRESSES Nxx FOR IDEALIZED BOUNDARY SERIES

Case	Edge Beam Stiffnesses *				Sketch of Nxx	Minimum Nxx	Maximum Nxx
	K1	K2	K3	K4	***	lbs/ft	lbs/ft
A	1	1	1	1	(a)	-665	
H	1	0	1	1	(a)	-672	
C	1	1	0	1	(a)	-674	
M	1	0	0	1	(a)	-674	
D	0	1	1	1	(b)	-652	+ 66
F	0	1	0	1	(b)	-661	+ 48
I	0	0	1	1	(c)	-677	
K	0	0	0	1	(c)	-673	
J	1	1	1	0	(d)	-995	
P	1	0	1	0	(d)	-1,010	
B	1	1	0	0	(d)	-1,024	
N	1	0	0	0	(d)	-1,024	
G	0	1	1	0	(e)	-1,010 ** -9,110	+ 2,500
E	0	1	0	0	(e)	-1,700 -10,500	+ 3,090
L	0	0	1	0	(f)	-1,370 -14,680	+ 1,420
Q	0	0	0	0	(f)	-1,320 -14,600	+ 1,390

* 1 Denotes infinite stiffness; 0 denotes zero stiffness.

** Local minimums.

*** See FIGURE 4.2 for sketches of Nxx Stress Distribution.

are shown by the individual sketches in FIGURE 4.2.

For K4 infinite, and if the shells edges are prevented from deflecting in a direction normal to the shell's surface, by either K1 or K2 being infinite (Cases A, H, C, M), direct stresses parallel to and at the edge will be zero or very small (sketches a and b), as expected. If, however, both K1 and K2 are zero, one would predict the existence of direct stresses parallel to and at the edges. This in fact happens, and the distribution of Nxx stresses is almost uniform throughout the shell as shown in sketch c (Cases I, K). All these cases have maximum compressive stresses almost identical in magnitude to those of the shell having built-in boundaries (Case A), for which the value is 665 lbs/ft.

For K4 = 0, two Nxx patterns exist, and reflect the effect of the edge beam's axial stiffness parameter K1. If K1 = infinity (Cases J, P, B, N), direct stresses are zero at the edges, and the maximum compressive stress is 57% greater than that of Case A. These cases would appear to be the ones most closely approached in practice. If, however, K1 = 0, very large compressive stresses appear near the corner support, and large tensile stresses occur at the mid-edges. When the shell's edge is supported by transverse forces (Cases G, E), the maximum compressive stress is 16 times that of Case A, and 22 times greater if the shell's edge is unsupported (Cases L, Q). The

tensile stresses appear to develop somewhat similarly to those along the bottom edges of barrel shells, where the shell's edge acts as a deep beam.

All cases yield identical compressive stresses of 625 lb/ft. at the crown, the value also given by the membrane analysis. A sketch of the Nxx distribution for the membrane analysis is given in FIGURE 5.5. Of the 16 combinations presented, Cases J, P, B and N appear to most closely resemble the membrane solution, but a marked difference occurs very near the edge that is parallel to the direction of the stress considered.

4.4 Bending Moments Mxx

The bending moments Mxx along the crown of the shell at $y = 0$, for various groups of edge beam stiffness combinations are presented in FIGURE 4.3. TABLE 4.4 gives the maximum and minimum values of the bending moments, which in all but a few cases occur on or very near to the corner of the shell.

To describe the types of Mxx distribution patterns that exist, qualitative sketches are given in FIGURE 4.4. In the discussion that follows, only moments in the vicinity of the edge $x = a$ are considered, unless otherwise noted.

All bending moment distribution patterns can be grouped into two main types. For those shells having torsionally stiff edge beams (K3 = infinity), bending moments exist at the edge,

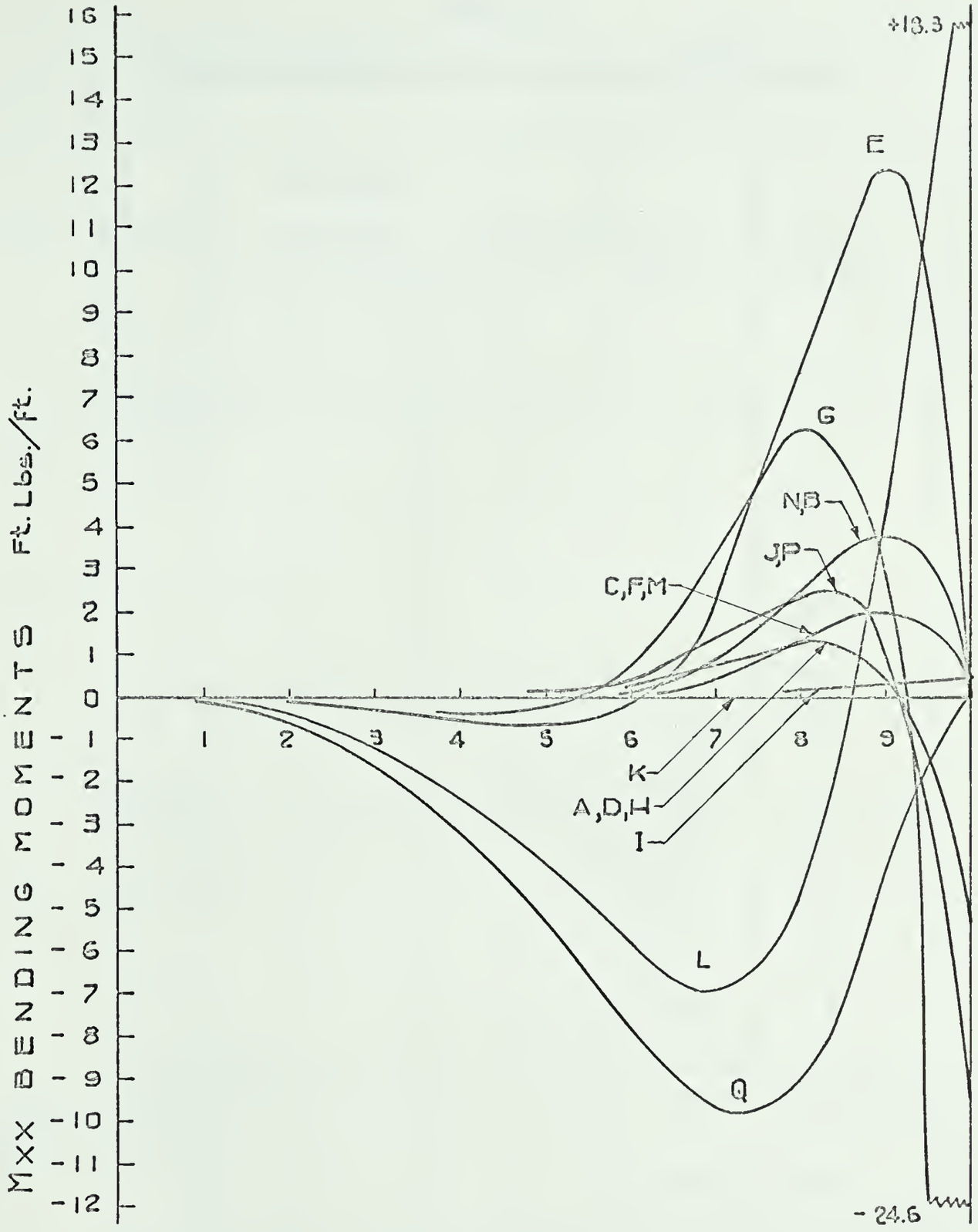

FIGURE 4.3 BENDING MOMENTS Mxx ALONG Y = 0
FOR IDEALIZED BOUNDARY SERIES

TABLE 4.4

BENDING MOMENTS Mxx FOR IDEALIZED BOUNDARY SERIES

Case	Edge Beam Stiffnesses (1)				Sketch (2)	Minimum Mxx (3)	Maximum Mxx (3)
	K1	K2	K3	K4			
K	0	0	0	1	(a)	0	1.47
F	0	1	0	1	(b)	0	2.02
C	1	1	0	1	(b)	0	2.17
M	1	0	0	1	(b)	0	2.17
B	1	1	0	0	(b)	0	3.84
N	1	0	0	0	(b)	0	3.84
H	1	0	1	1	(c)	-0.92	6.85
P	1	0	1	0	(c)	-1.36	12.6
I	0	0	1	1	(d)	-4.06	1.05
D	0	1	1	1	(e)	-5.43	1.31
A	1	1	1	1	(e)	-5.67	1.39
J	1	1	1	0	(e)	-9.69	2.34
G	0	1	1	0	(e)	-24.6 (4)	6.30 (4)
E	0	1	0	0	(b)	-4.25	12.3 (4)
L	0	0	1	0	(f)	-36.6	89.8
Q	0	0	0	0	(g)	-51.3	25.7 (5)

(1) 1 Denotes infinite stiffness; 0 denotes zero stiffness

(2) See FIGURE 4.5 for sketches of Mxx distribution patterns.

(3) Occur near or at corner of shell, except as noted.

(4) Occurs on crown line y = 0.

(5) Occurs at mid-edge y = a.

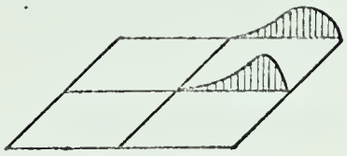

a) Cases C,F,M,B,N,E.

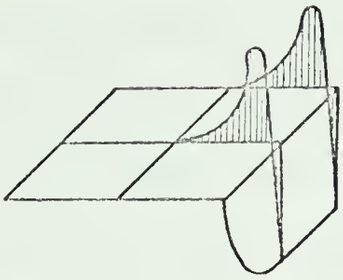

b) Cases A,D,J,G.

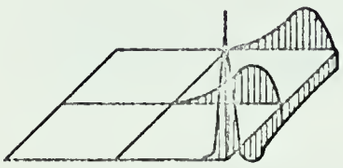

c) Cases H,P.

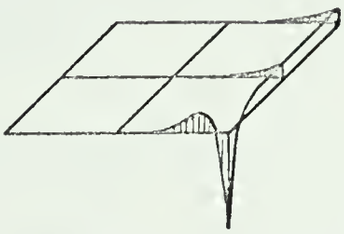

d) Case I.

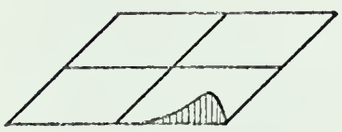

e) Case K.

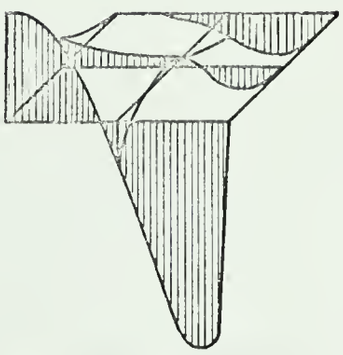

f) Case Q.

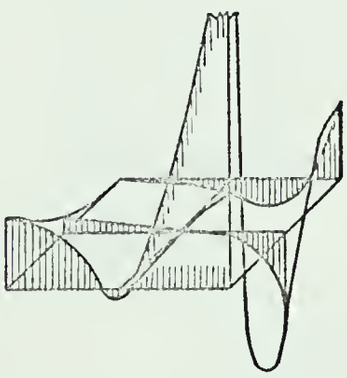

g) Case L.

Axes :

The sketches are to scale for first Case in each list. Refer to TABLE 4.4 for maximum Mxx values.

Scales: I = 500 Ft. Lbs./ft.
(= 2500 Cases Q, L.)

FIGURE 4.4 BENDING MOMENT Mxx DISTRIBUTIONS FOR IDEALIZED BOUNDARY SERIES

but when the edge is torsionally unrestrained (K3 = 0), they cannot exist at the edge. Thus the primary effect of K3 on Mxx distributions and magnitudes is recognized, and can be seen in FIGURE 4.4. Within these two clearly defined Mxx distribution types, considerable variations in magnitude and distribution occur in the shell, depending on the variations in the remaining stiffnesses. These variations are somewhat complex, and groupings do not appear as clearly in moments as in other effects.

The mechanisms by which the shell derives support at the boundaries greatly affect bending moments. Considering the Cases A, D, I, H, M, C, F and K, wherein compressive stresses across the edge are the main load carrying mechanism, the transverse bending moments are low, ranging from -5.67 to 6.85 ft.lbs/ft. Case A, the shell having built-in boundaries, has a range of -5.67 to 1.39 ft.lbs/ft. Within this group, for K3 = 0, maximum moments are less than 2.17 ft.lbs/ft. Changing K2 from 0 to infinity has the effect, very roughly, of increasing the maximum moments by a factor of about 1.3 times. K1 has a lesser effect on moments. The Mxx distribution patterns vary considerably, as can be seen in FIGURE 4.4.

As previously stated, K4 has considerable effect on Mxx. Thus, provided K1 = infinity, changing K4 from zero to infinity increases the maximum bending moments by 1.7 times (Cases A-J, M-N, B-C, H-P). Similarly, for K1 = zero, changing K4 has a considerable effect, as shown by Cases D-G, E-F, K-Q, and I-L,

where Mxx is increased from 4.8 times to 85 times, depending on what other edge restraints are active. It is evident, therefore, that in-plane forces, either Nxx or Nxy, must exist at the shell's edge (ie K1 or K4 must be large) to keep maximum bending moments within reasonable limits.

When transverse forces, but not in-plane forces, exist at the edge (Cases E and G), the bending moments become large. If in-plane and transverse forces cannot exist at the boundaries, extremely large bending moments develop.

The sketches shown in FIGURE 4.4 indicate the complex Mxx distribution patterns that arise. The type of distribution, and to a generally much lesser extent the magnitudes within the types, appear to depend on the combination of stiffnesses K2 and K3. Thus, for all combinations with K2 = K3 = infinity (Cases A, D, J, G), the Mxx distributions are of the type shown in sketch (b), whereas sketch (a) is representative of the Mxx distributions in the combinations having K2 = infinity and K3 = 0 (Cases B, C, E, F). For K2 = K3 = 0 (Cases M, N, K, Q), the bending moments are small (excluding Case Q which has free boundaries), and of the distribution type shown in sketches (a), (e) and (f).

Rather complex Mxx patterns exist, shown in sketches (c) (d) and (g), when K2 = 0 and K3 = infinity (Cases H, I, L, and P). This results from the academic effect of framing at the corner a torsionally stiff edge beam into the perpendicular edge beam, which has no flexural stiffness. It appears that when K2 = 0, a torsional restraint must exist at the corner support if the beam

is to be torsionally restrained. Interestingly enough, this problem became evident in the computer solutions, where round-off error became excessive if K3, in order to approximate infinity, was made excessively large, say 10^{15}, but reasonable results were obtained when K3 was set at 10^{5}.

It was found that for most of the cases represented by sketches (a) and (b), the maximum positive values of Mxx, which occur near the corner but are not shown in the sketches, are at most 11% greater than the maximum positive moment on the crown line y = 0, shown in FIGURE 4.3 FIGURE 4.3 also indicates that for cases where in-plane forces or transverse forces exist (all Cases except Q and L), the positive bending moments peak within a distance of about 0.2a from the edge, and rapidly diminish to zero within 0.4a from the edge.

4.5 Shear Stress Resultants Nxy

The shear stress resultants Nxy, also referred to as shear forces, are presented in FIGURE 4.5 for the line x = 9.5 or y = 9.5. Maximum calculated values of Nxy are given in TABLE 4.5.

It is to be noted that the shear resultants are defined at secondary grid points, which are midway between the primary grid points. Thus the Nxy resultants plotted in FIGURE 4.5 are a half-grid spacing removed from the edge of the shell. Since

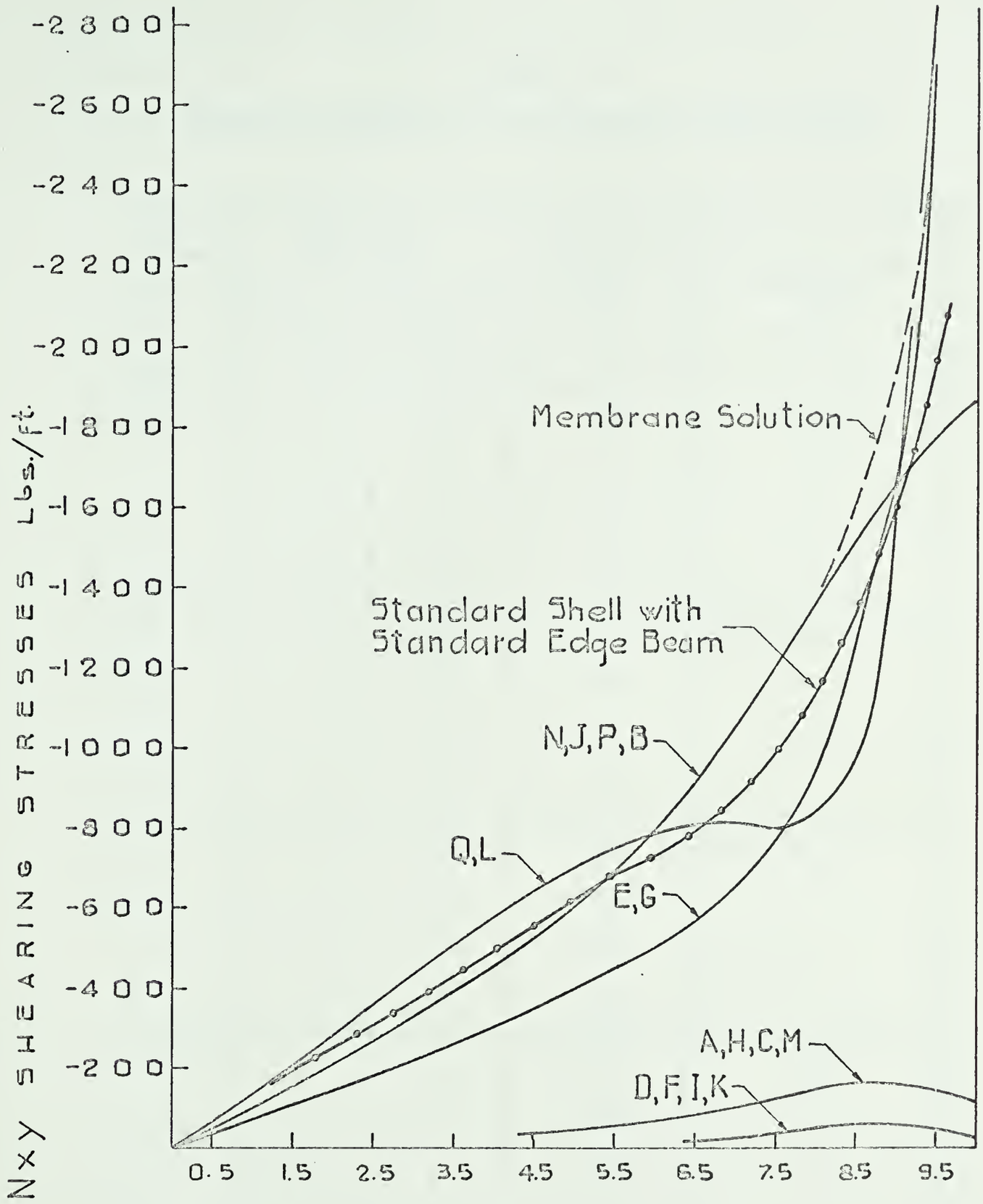

FIGURE 4.5 SHEARING STRESSES Nxy ALONG X = 9.5
FOR IDEALIZED BOUNDARY SERIES

TABLE 4.5

SHEARING STRESSES Nxy FOR IDEALIZED BOUNDARY SERIES

Case	Edge Beam Stiffnesses *				Maximum Calculated Shear	Theoretical Shear at Edge
	K1	K2	K3	K4	lbs/ft	lbs/ft
K	0	0	0	1	-46	Zero
I	0	0	1	1	-61	"
F	0	1	0	1	-67	"
D	0	1	1	1	-87	"
A	1	1	1	1	-155	Not Zero
H	1	0	1	1	-176	" "
C	1	1	0	0	-175	" "
M	1	0	0	1	-175	" "
J	1	1	1	0	-1524	Not Zero
P	1	0	1	0	-1789	" "
B	1	1	0	0	-1786	" "
N	1	0	0	0	-1786	" "
G	0	1	1	0	-2480	Zero
E	0	1	0	0	-2820	"
Q	0	0	0	0	-2858	"
L	0	0	1	0	-3011	"

* 1 denotes infinite stiffness; 0 denotes zero stiffness

the shearing forces generally increase toward the edge, and generally increase rapidly toward the corner of the shell, the calculated values do not give a clear indication of the actual maxmimum values of Nxy. This is expecially true for Cases G, L, E and Q, in which the shearing forces are known to be zero at the edge because the axial stiffness (K1) of the edge beam is zero, yet the indicated values 0.05a from the edge are very high. Thus the maximum value of Nxy is not known.

Four distinct behaviour groups are evident. The first group (Cases K, I, F, D), for which the in-plane bending stiffness of the edge beam (K4) is infinity, and for which K1 is zero, exhibit very low shearing stresses, which diminish to zero along the edges. The maximum magnitude of Nxy is in the order of half that of the shell having built-in edges, Case A. Shearing stresses for this group are not significant because the main load carrying mechanism of the shell consists of in-plane compressive forces across the edge.

If, in the preceding group, the stiffness K1 is made very large (Cases A, C, H, M), the maximum Nxy stresses are roughly doubled, but still very low (155 lbs/ft. for Case A). Nxy stresses along the edge are not zero. Again, the direct stresses acting across the edge predominate and shearing stresses are insignificant.

When direct stresses across the edges cannot exist (K4 = 0), but K1 = infinity, in-plane shearing stresses along the

edge become the significant support mechanism. Thus, for Cases J, P, B, and N, the maximum calculated values of Nxy increase tenfold over Case A. This group appears to represent most closely the type of edge member that is practical to construct, as will be shown in CHAPTER V. The membrane analysis, also shown on FIGURE 4.7, yields results similar to this group, except very near the corner, where it indicates much higher Nxy values.

When both K1 and K4 are zero (Cases G, E, Q, L), in-plane forces cannot be transmitted to the edge member, and the maximum value of Nxy is increased by a factor of 16 to 19 times that of Case A, clearly an undesirable situation.

The torsional stiffness (K3) and the transverse bending stiffness (K2) of the edge beam, which considerably affect bending moments near the shell's boundaries, have little effect on the shearing stresses.

4.6 Twisting Moments Mxy

Twisting moments Mxy along x = .95a or y = .95a are given in FIGURE 4.6. Mxy moments are defined at the same locations as shearing forces, and the same uncertainties exist regarding locations and magnitudes of maximum values. The magnitudes of twisting moments are generally in the same order, or less, than bending moments. Four behaviour groups are evident in FIGURE 4.6 and in TABLE 4.6, which contains maximum calculated values of Mxy.

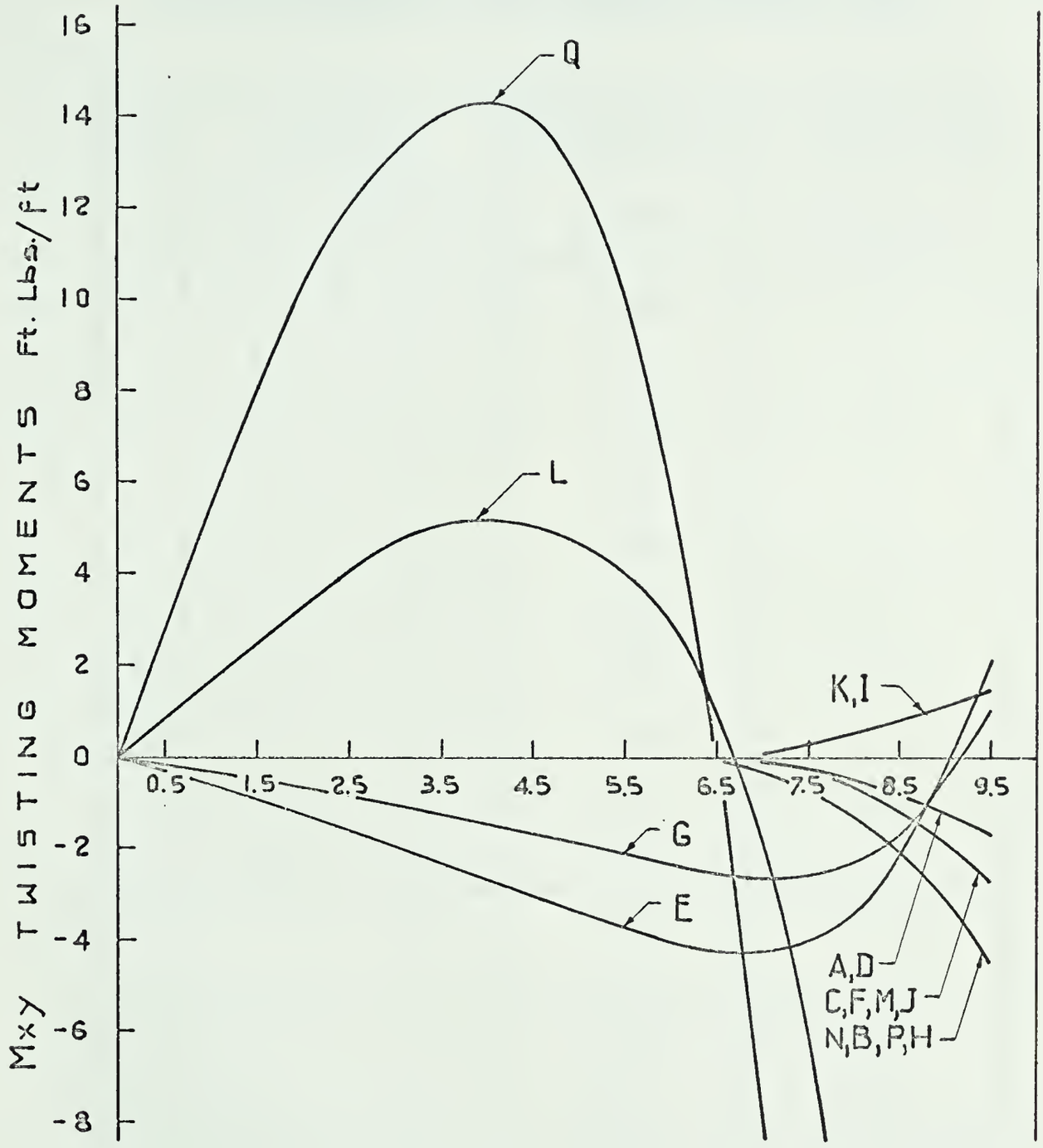

FIGURE 4.6 TWISTING MOMENTS Mxy ALONG X = 9.5
FOR IDEALIZED BOUNDARY SERIES

TABLE 4.6

TWISTING MOMENTS Mxy FOR IDEALIZED BOUNDARY SERIES

Case	Edge Beam Stiffnesses *				Calculated Mxy at x=y=0.95a **	Maximum Mxy of Opposite Sign
	K1	K2	K3	K4	ft.lbs/ft	ft.lbs/ft
D	0	1	1	1	-1.38	0
A	1	1	1	1	-1.62	0
F	0	1	0	1	-2.39	0
J	1	1	1	0	-2.47	0
C	1	1	0	1	-2.68	0
M	1	0	0	1	-2.68	0
H	1	0	1	1	-2.79	0
B	1	1	0	0	-4.42	0
N	1	0	0	0	-4.42	0
P	1	0	1	0	-4.86	0
I	0	0	1	1	+1.31	0
K	0	0	0	1	+1.55	0
G	0	1	1	0	+1.02	-2.64
E	0	1	0	0	+2.11	-4.26
L	0	0	1	0	-33.9	+9.70
Q	0	0	0	0	-61.4	+14.7

* 1 Denotes infinite stiffness; 0 denotes zero stiffness.

* These are also the maximum calculated values, except for Cases G and E.

The main group (Cases D, A, H, C, M, P, B, N, J and F) has Mxy moments that diminish from a maximum negative value at the corner to zero within 0.35a from the corner. In this group, transverse and in-plane forces act at the edge and large twisting moments do not develop.

The second group (Cases K, I) reveals twisting moments similar in magnitude but reversed in sign to the first group. For these cases the shearing and transverse forces are zero at the edge, the primary support mechanism of the shell being direct forces across the edge.

In the third group (Cases E, G), only transverse forces are present at the edge, with the resulting twisting moments extending over the complete shell.

The last group (Cases Q, L) has very large Mxy magnitudes, and the distribution is similar, but reversed in sign, to the third group.

The effects on Mxy of changing individual stiffness parameters can be seen by taking the stiffness combination relationships given in TABLE 4.1 and applying them to TABLE 4.6. This shows, for example, that changing K3 from infinity to 0 for the stiffness combinations A-C, D-F and D-J has the effect of increasing Mxy moments by about 1.8 times. Other effects become apparent in a similar manner.

4.7 Summary

In the preceding sections only idealized values of the stiffness parameters were considered, ie zero or infinity. Since values were assigned arbitrarily in all combinations without regard to the physical problems of obtaining these combinations, the effects of each parameter is exaggerated thus making interpretation easier. It would appear that the four stiffness parameters can be ranked in order of predominance on their effect on shell behaviour.

If K4 = infinity, ie no outward in-plane movement permitted at the edge, then the load is carried almost solely by membrane action as direct stress, that is arching to the edges, with little or no bending for uniformly distributed loads. The values assigned to the other parameters are relatively unimportant.

If K4 = 0 the next important parameter is K1. Again the load is carried predominantly by membrane action, this time as in-plane shearing stress but deformations are somewhat greater.

If both K1 and K4 are zero, the load is carried by beam action and bending moments are important. For K2 = infinity, the effect of K3 is small and restricted to the immediate vicinity of the edge. For K2 = 0, deflections and stresses become large, as the shell is unsupported at the edges.

CHAPTER V

SHELLS SUPPORTED BY ELASTIC EDGE BEAMS

5.1 Introduction

To obtain qualitative insight into the behaviour of shells with boundaries consisting of elastic edge beams, the stiffness parameters were evaluated for three series of shells. In one series the effect on the shell of varying the size of the square edge beam from a free edge condition through to an infinite stiffness condition was evaluated. In a second series the shape of the edge beam of constant area was varied from a deep narrow shape through to a wide shallow shape to determine the effect on the shell. For a third series, the edge beam was held to a constant shape and size, and the effects of varying the rise of the shell was evaluated. The discussions that follow deal more with the practical range of size and shape factors, but the limiting conditions are also presented to allow comparisons to be made with the idealized boundary condition series presented in CHAPTER IV. All three series include the "standard shell" having the "standard edge beam", which are defined in CHAPTER III, to allow conclusions drawn from one series to be qualitatively extended into another series.

The results are presented in the order of normal deflections, direct stress resultants, bending moments and shearing stresses.

5.2 Normal Deflections for Shells Supported by Elastic Edge Beams

The magnitudes of the normal deflections at the crown, the mid-edge, and the maximum upward deflection near the corner, for all shells discussed in this chapter, are given in TABLE 5.1.

5.2.1 Size of Edge Beam Series

Normal deflections along the crown line are shown in FIGURE 5.1, and the normal deflections along the edge in FIGURE 5.2. The magnitude and pattern of the normal deflections for shells with very large edge beams or no edge beams are identical to those of Cases A (built-in boundaries) and Q (free edges) respectively, which are discussed in CHAPTER IV. The standard shell with the standard edge beams (See CHAPTER III for description) deflects similarly to Case G (K1 = K4 = 0, K2 = K3 = infinity) in the central region of the shell, with the crown deflection larger by 1% for the standard shell. However, at the mid-edge, where Case G does not deflect, the standard shell deflects 53% more than at the crown, and deflects upward near the corner support to 42% of the crown deflection.

For the practical range of edge beam sizes considered, K1 and K2 are the only stiffnesses that have any significant effect on the general deflection behaviour. For b = d = 10t (the cross-sectional dimensions of the edge beam), the deflection magnitude in the central region of the shell is similar to that of Cases J, P, B and N, but approaches that of Cases G and E when b = d = 4t. This appears to indicate that as the size of the beam is decreased the effect of K2 becomes increasingly important relative to K1.

TABLE 5.1

NORMAL DEFLECTIONS FOR SHELLS SUPPORTED BY ELASTIC EDGE BEAMS

		Crown Deflection x 10,000	Mid-Edge Deflection x 10,000	Maximum * Upward Deflection x 10,000
Size of Edge Beam Series	d = b = 1000t	0.86a	0	0
	100t	0.86a	0	0
	10t	1.75a	0.54a	0
	8t	1.91a	0.90a	0
	6t	2.25a	1.81a	0.14a
	Standard 4t	3.37a	5.18a	1.43a
	2t	8.48a	21.6a	10.8a
	0t	13.3a	35.4a	20.0a
Shape of Edge Beam Series	d:b = 1.000:1	2.28a	0.30a	0
	3:1	2.86a	3.15a	0.27a
	2:1	3.01a	3.74a	0.60a
	Standard 1:1	3.37a	5.18a	1.43a
	1:2	3.90a	7.19a	2.69a
	1:3	4.28a	8.62a	3.71a
	1:1000	2.12a	3.15a	2.16a
Variation of Rise to Span Ratio Series	h/a = 0.24	1.93a	3.95a	1.74a
	0.20	2.46a	4.40a	1.61a
	Std. 0.16	3.37a	5.18a	1.43a
	0.12	5.35a	6.81a	1.02a
	0.08	10.9a	11.2a	0.08a
	0.04	41.6a	33.5a	0
	0.000025	3270a	1460a	0

* Occurs near the corner of the shell

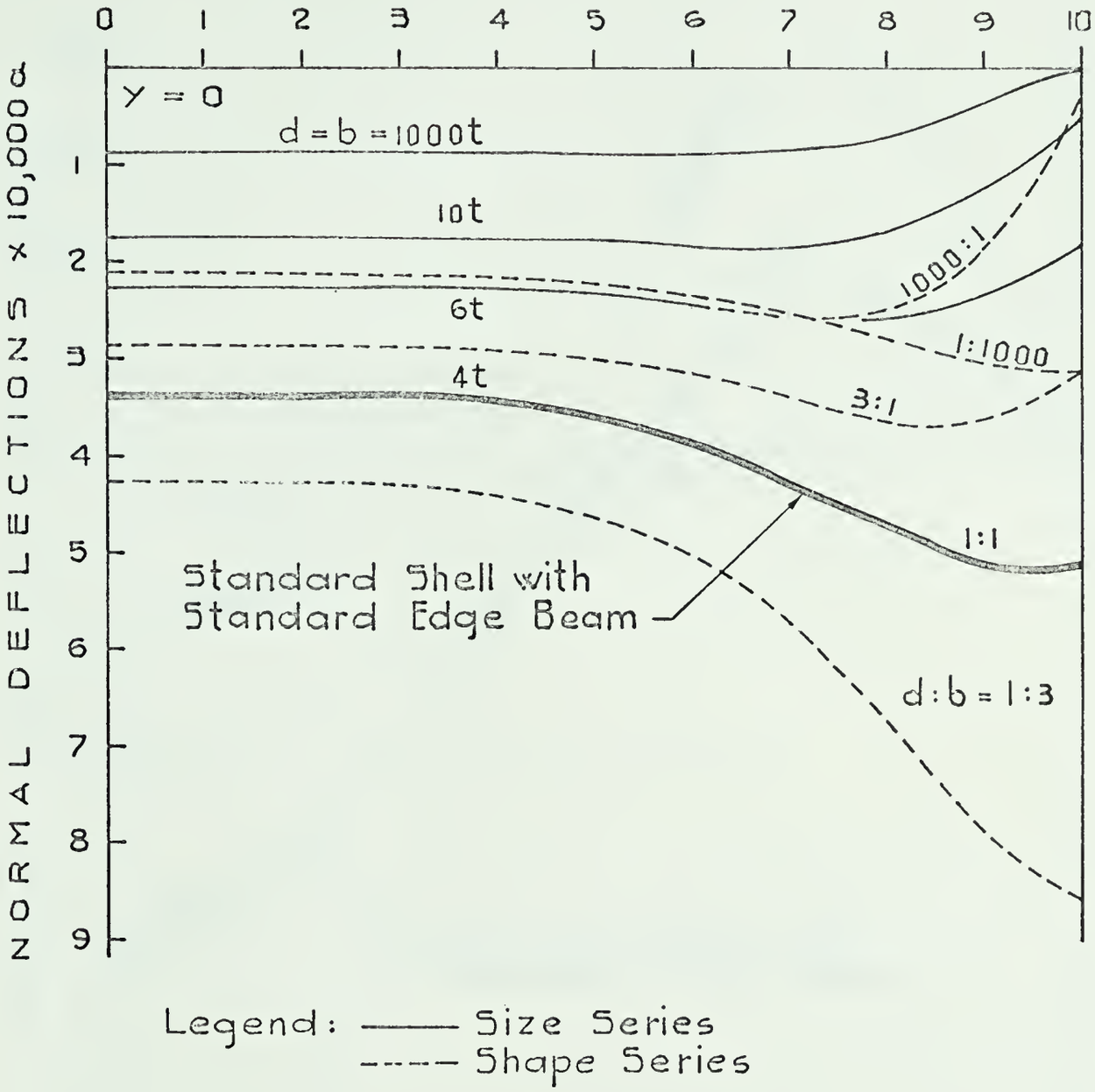

FIGURE 5.1 NORMAL DEFLECTIONS ALONG CROWN LINE FOR SIZE OF EDGE BEAM SERIES AND SHAPE OF EDGE BEAM SERIES

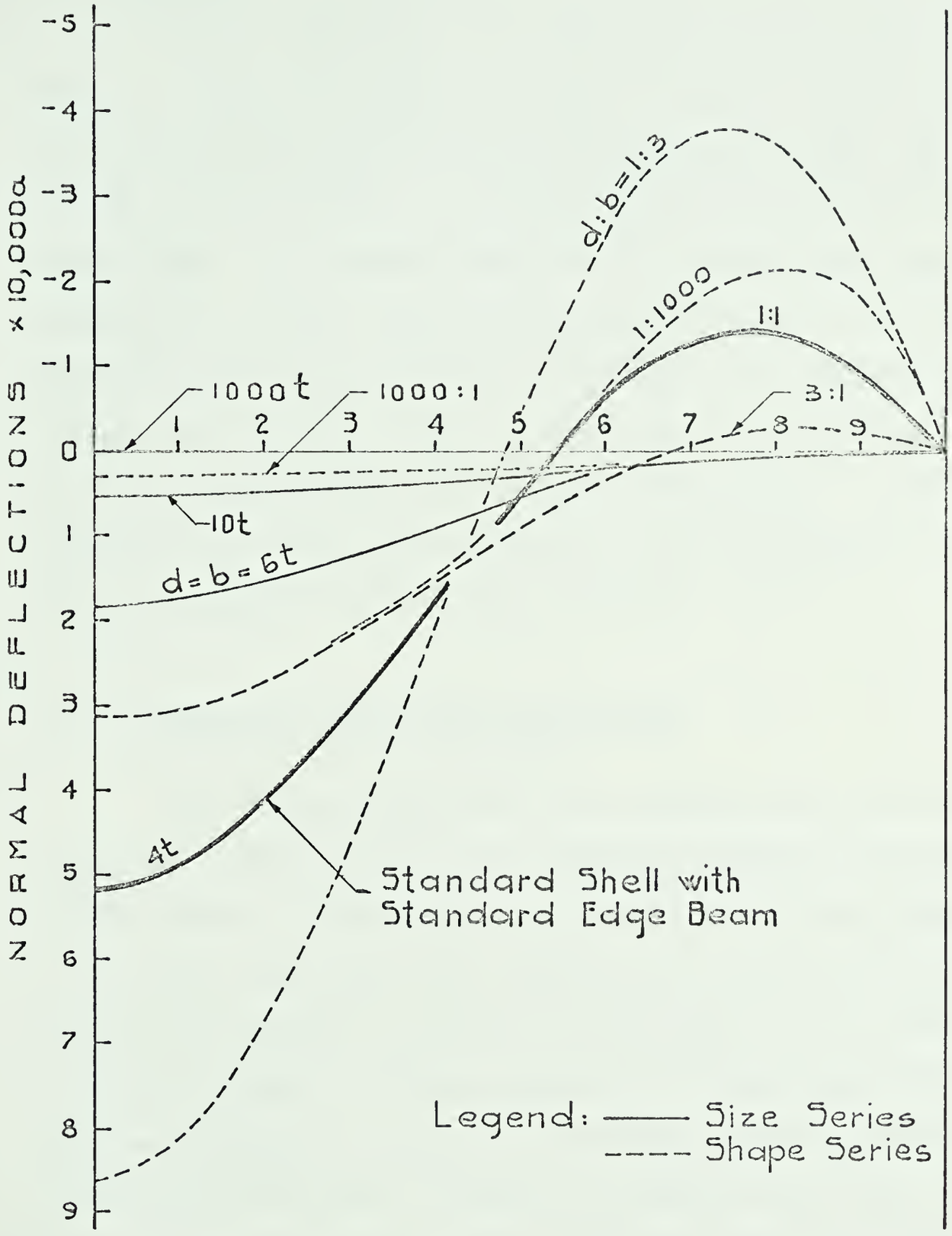

FIGURE 5.2 NORMAL DEFLECTIONS ALONG EDGE FOR SIZE OF EDGE BEAM SERIES AND SHAPE OF EDGE BEAM SERIES

5.2.2 Shape of Edge Beam Series

Normal deflections of the shell along the crown line and along the edge are also given in FIGURES 5.1 and 5.2. For the five practical depth:width (d:b) ratios studied, the normal deflections decrease as d:b increases. This effect is more pronounced at the shell's edge. For instance, with d:b = 3:1 the shell's mid-edge deflects only slightly more than the centre, but for d:b = 1:3 the mid-edge deflects twice as much as the centre. This indicates the primary effect, on deflections, of transverse forces along the edges, for these particular shell and edge beam configurations. There is no significant effect on deflections that can be attributed to K3 or K4 in the range of edge beam sizes presented.

5.2.3 Variation of Rise to Span Ratio Series

The deflection behaviour of the standard shell with standard edge beam is fairly typical of the deflection behaviour of the shells in this series. The deflections (see TABLE 5.1) increase hyperbolically as the rise to span ratio (h/a) decreases, but the deflection pattern does not alter except for the very shallow shells. In the latter case, the stiffness of the shell relative to the stiffness of the edge beam decreases, resulting in a decreasing edge-of-shell/centre-of-shell deflection ratio. When h/a is assigned a very small value, that is the shell becomes a plate, the central deflection is 1000 times larger than for the standard shell having the same edge beam size.

5.3 Direct Stress Resultants for Shells Supported by Elastic Edge Beams

Direct stress resultants Nxx for three locations in the shells are given in TABLE 5.2 These are the Nxx stresses at the corner, at the mid-edge x = 0, and the maximum Nxx value along the crown line x = 0. For the practical cases studied the Nxx distribution patterns are qualitatively similar, but the magnitudes vary considerably and are discussed further below. In all cases, except where the shell height was varied, the compressive stress at the crown was 625 lbs/ft. To give a clearer picture of the direct stresses, qualitative sketches are presented in FIGURES 5.3, 5.4 and 5.5. The membrane analysis is also given in FIGURE 5.5 for comparison purposes.

5.3.1 Nxx - Size of Edge Beam Series

The shell with built-in boundaries has an Nxx distribution pattern varying only slightly from uniform except along the edge y = a, where the direct stress is zero. As the size of the square edge member decreases to finite dimensions, the stress distribution becomes more complex as shown in FIGURE 5.3, and when the edge member size diminishes to a free edge condition, high stresses develop along the edge y = a, especially at the corner.

Maximum compressive Nxx stresses along the line x = 0 are 106%, 169% and 212% of the crown value of 625 lbs/ft. for the built-in, the standard, and the free edge cases, respectively. At the mid-edge y = a the compressive stresses, which are small, reverse

TABLE 5.2

DIRECT STRESSES Nxx FOR SHELLS SUPPORTED BY ELASTIC EDGE BEAMS

		Nxx at Crown lbs/ft.	Max. Nxx along y=0 lbs/ft.	Nxx at y=a,x=0 lbs/ft.	Nxx at Corner lbs/ft.
Size of Edge Beam Series	d = b = 1000t	-625	-665	0	0
	100t	"	-666	0	0
	10t	"	-969	-18	-671
	8t	"	-975	-23	-1071
	6t	"	-987	- 9	-1875
	Standard 4t	"	-1053	+101	-3742
	2t	"	-1251	+701	-8521
	0t	"	-1324	+1391	-14560
Shape of Edge Beam Series	d:b = 1000:1	-625	-1059	+866	-2927
	3:1	"	-1031	+105	-3760
	2:1	"	-1036	+ 99	-3758
	Standard 1:1	"	-1053	+101	-3742
	1:2	"	-1091	+133	-3704
	1:3	"	-1120	+164	-3673
	1:1000	"	-707	-189	-1413
Variation of Rise to Span Ratio Series	h/a = 0.24	-418	-746	+123	-2504
	0.20	-500	-876	+118	-2999
	Std. 0.16	-625	-1053	+101	-3742
	0.12	-830	-1338	+ 59	-4977
	0.08	-1244	-1926	- 44	-7429
	0.04	-2612	-3530	-260	-14520

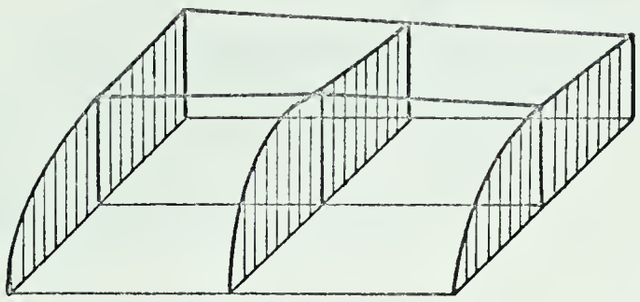

d = b = 1000t

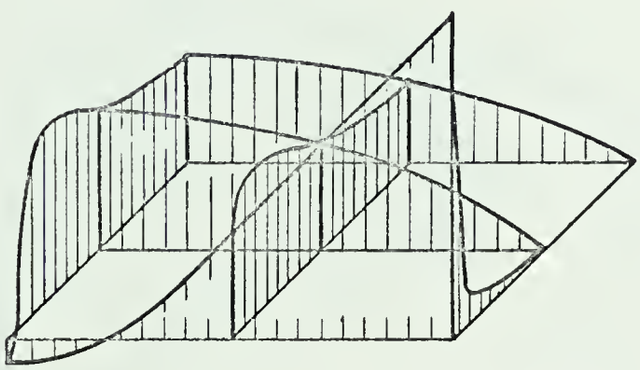

d = b = 4t Standard Shell with Standard Edge Beams.

Refer to TABLE 5.2 for values of Nxx.

Scale : I - 500 Lbs./ft.

Axes : x, y, z

FIGURE 5.3 DIRECT STRESS Nxx DISTRIBUTIONS FOR SIZE OF EDGE BEAM SERIES

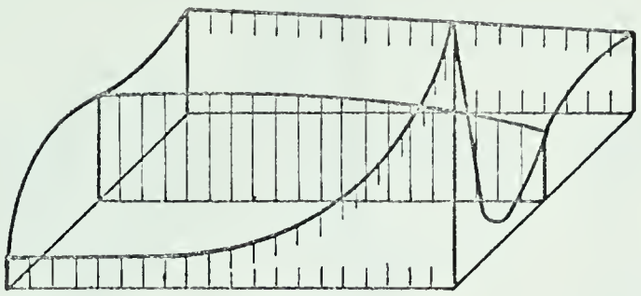

d = b = 1 : 1000

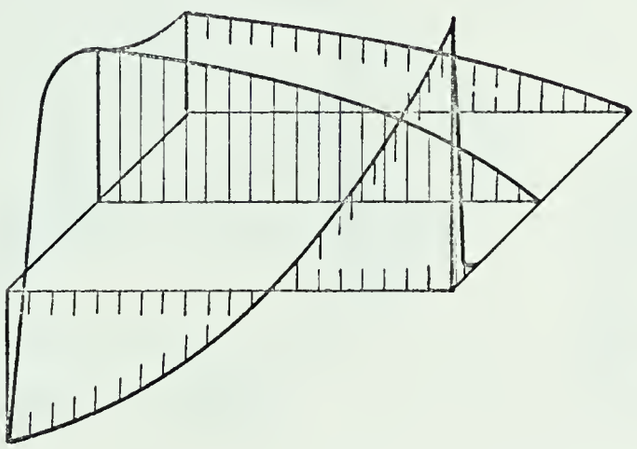

d = b = 1000 : 1

Refer to TABLE 5.2
for values of Nxx.

Scale : ⟷ 500 Lbs/ft.

Axes : x, y, z

FIGURE 5.4 DIRECT STRESS Nxx DISTRIBUTIONS
FOR SHAPE OF EDGE BEAM SERIES

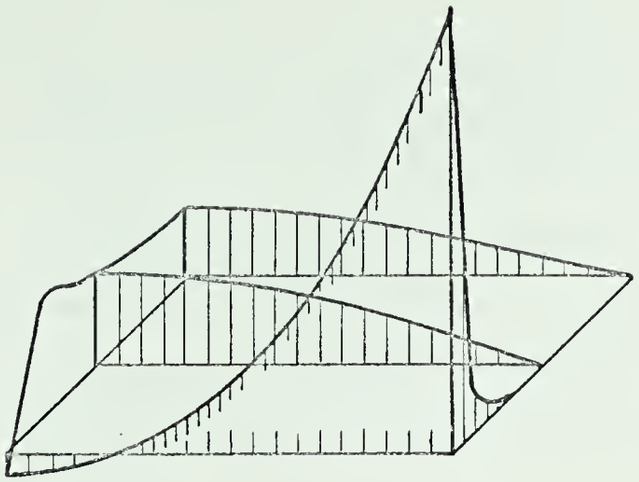

h/a = 0.24

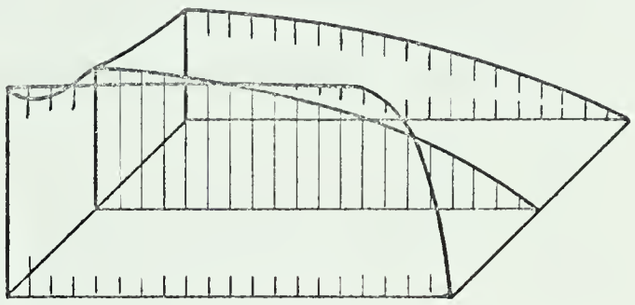

Membrane Solution
h/a = 0.16

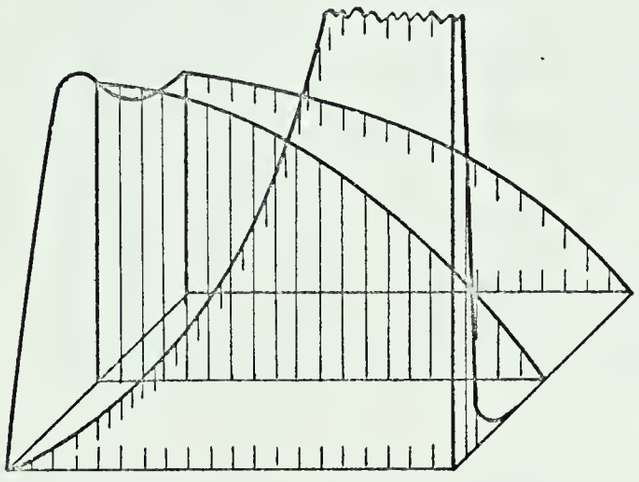

h/a = 0.08

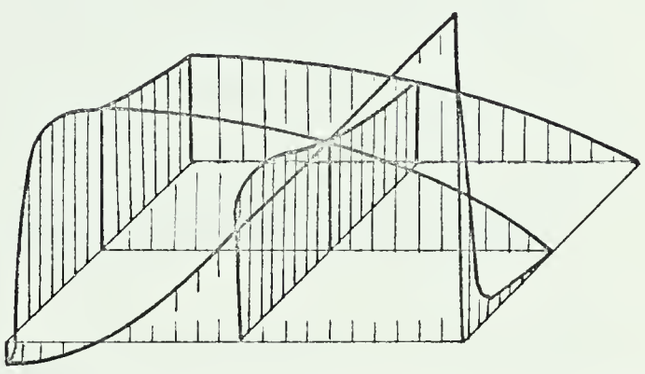

Standard Shell h/a = 0.16

Refer to TABLE 5.2
for values of Nxx.

Scale :  - 500 Lbs./ft.

Axes : 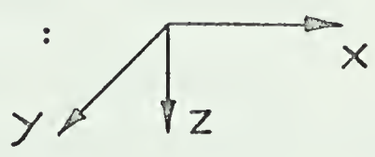

FIGURE 5.5 DIRECT STRESS Nxx DISTRIBUTIONS
FOR VARIATION OF RISE TO SPAN RATIO SERIES
AND MEMBRANE ANALYSIS

when the edge member dimension decreases below 6t, and become large tensile forces for the free edge case, in the case considered 1391 lbs/ft. Decreasing the size of the edge member becomes even more noticeable in its effect on Nxx in the vicinity of the corner. Here compressive stresses of 23 times the crown value are obtained as the shell is forced to pick up the total load for the free edge condition.

The shells with edge beams of practical sizes have similar stress behaviour to a hypothetical case between the group having edge beams with large axial stiffnesses (Cases J, P, B, N) and the group with edge beams having large transverse bending stiffnesses (Cases G and E), which are presented in CHAPTER IV. Actually, the shells of this series behave very closely to Cases J, P, B and N, except near the corner where they behave more like Cases G and E.

5.3.2 Nxx - Shape of Edge Beam Series

As shown in TABLE 5.2, changing the shape, of the constant area edge beams, within a practical range, has no significant effect on Nxx stresses. Changing the d:b ratio of the edge beams from 3:1 to 1:3 increases the maximum compressive stress in the shell's interior region by only 9% and decreases them at the corner by 3%.

Within the practical range of d:b ratios, the in-plane stiffness parameter K4 has no apparent effect. This appears reasonable since the in-plane stiffness of the shell overwhelms the stiffness of the edge beam.

The shape of the edge member in a practical situation would probably be adjusted more in consideration of other effects, such as bending stresses, rather than Nxx stresses. This is discussed in later sections.

5.3.3 Nxx - Variation of Rise to Span Ratio Series

The maximum and minimum Nxx stress resultants at key locations in the shell for varying h/a ratios are presented in TABLE 5.2. The magnitude of Nxx at the crown is as predicted by membrane theory, except for slight variations for the very shallow shells with h/a less than 0.04. It is to be noted that for this series having a square edge beam configuration, the maximum compressive stresses, which occur at the corner, are almost exactly 6 times as large as the compressive stresses at the crown. There is a slight decrease in this ratio for the shallowest shell studied in which h/a = 0.16.

5.4 Bending Stresses Mxx

TABLE 5.3 gives the calculated values of the bending moments Mxx at seven key locations in the shell, for all three series of edge member and shell configurations. The key locations are identified in FIGURE 5.6. Locations 3,5 and 7 are "fixed locations" at the mid-edge x = a, corner, and mid-edge y = a, respectively. Locations 1, 2, 4 and 6 are "floating locations", that is they shift positions as the parameters are varied. For

TABLE 5.3

BENDING MOMENTS Mxx FOR SHELLS SUPPORTED BY ELASTIC EDGE MEMBERS

Location (See FIG. 5.6)		1 *	2	3	4	5	6	7
Size of	d=b= 1000t	-0.03	1.25	-5.15	-5.68	0.00	0.00	0.00
Edge Beam	100t	-0.04	1.26	-5.18	-5.68	0.00	0.00	0.00
Series	10t	-0.12	2.15	-7.39	-7.39	0.07	-0.08	0.16
	8t	-0.14	2.04	-6.12	-6.29	0.14	-0.23	0.33
	6t	-0.27	2.02	-3.69	-5.27	0.33	-0.83	0.88
	Std. 4t	-1.00	2.67	1.39	-7.40	1.34	-4.07	3.39
	2t	-5.89	3.96	3.96	-9.45	12.5	-26.5	16.4
	0t	-9.65	0	0	0	0	-51.3	25.7
Shape of	d:b=1000:1	-0.32	6.15	-0.01	-0.01	0.00	0.05	0.05
Edge Beam	3:1	-0.51	3.09	-0.12	-2.35	0.15	-1.60	1.56
Series	2:1	-0.64	2.92	0.21	-3.88	0.37	-2.30	2.09
	1:1	-1.00	2.67	1.39	-7.40	1.34	-4.07	3.39
	1:2	-1.54	3.63	3.63	-11.5	3.57	-6.77	5.22
	1:3	-1.99	5.14	5.14	-13.7	5.66	-8.89	6.50
	1:1000	-0.50	0.88	0.01	-0.31	1.04	-10.1	1.43
Variation	h/a = 0.24	-1.10	2.58	2.58	-8.69	1.43	-3.95	3.08
of Rise to	0.20	-0.98	2.07	2.07	-8.06	1.39	-4.01	3.20
Span Ratio	Std. 0.16	-1.00	2.67	1.39	-7.40	1.34	-4.07	3.39
Series	0.12	-0.93	3.43	0.50	-6.60	1.27	-4.11	3.73
	0.08	-0.89	4.57	-0.53	-5.37	1.13	-4.02	4.55
	0.04	-0.75	8.86	-0.18	-3.71	0.74	-2.96	8.20

* Bending Moments are ft.lbs/ft.

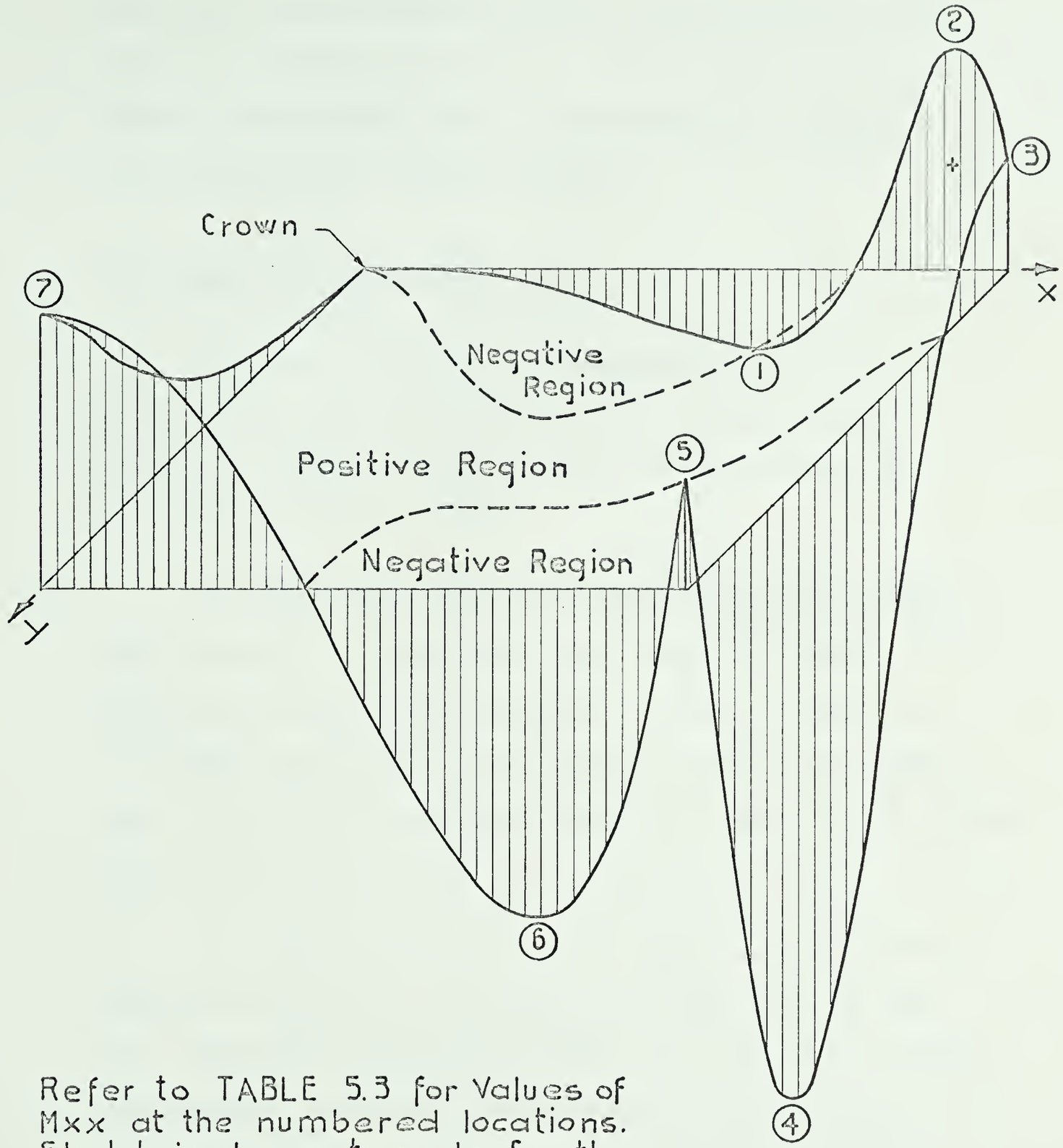

Refer to TABLE 5.3 for Values of Mxx at the numbered locations. Sketch is drawn to scale for the Standard Shell with Standard Edge Beams.

FIGURE 5.6 BENDING MOMENT Mxx DISTRIBUTIONS FOR SHELLS SUPPORTED BY ELASTIC EDGE BEAMS

each series, bending moments at the key locations indicated are plotted, in FIGURES 5.7, 5.8 and 5.9. These figures show the trends in the magnitude of Mxx as the parameters are varied, and are discussed in the following sections.

5.4.1 Mxx - Size of Edge Beam Series

The values of Mxx at seven key locations, which are generally local maximum or minimum values in the shell, are presented in FIGURE 5.7 for this series, in which the size of the square edge beam was varied.

For large edge beams, the bending moments are generally small, whereas for the shell with a free edge, the bending moments become high at a few locations. As shown in FIGURE 5.7 by the dashed vertical line, there exists a size of square edge beam, with side dimensions of approximately 7t, for which the greatest value of Mxx at any location in the shell is a minimum.

For the shell with this optimum edge beam size Mxx has a maximum value of about -5. ft.lbs/ft. and occurs along the edge x = a. Decreasing the size of the edge beam to 4t, ie the standard edge beam size, the largest bending moment increases by 40% to -7.40 ft.lb/ft. Decreasing the size of the edge beam beyond 4t results in rapidly increasing bending moments, a highly undesirable situation.

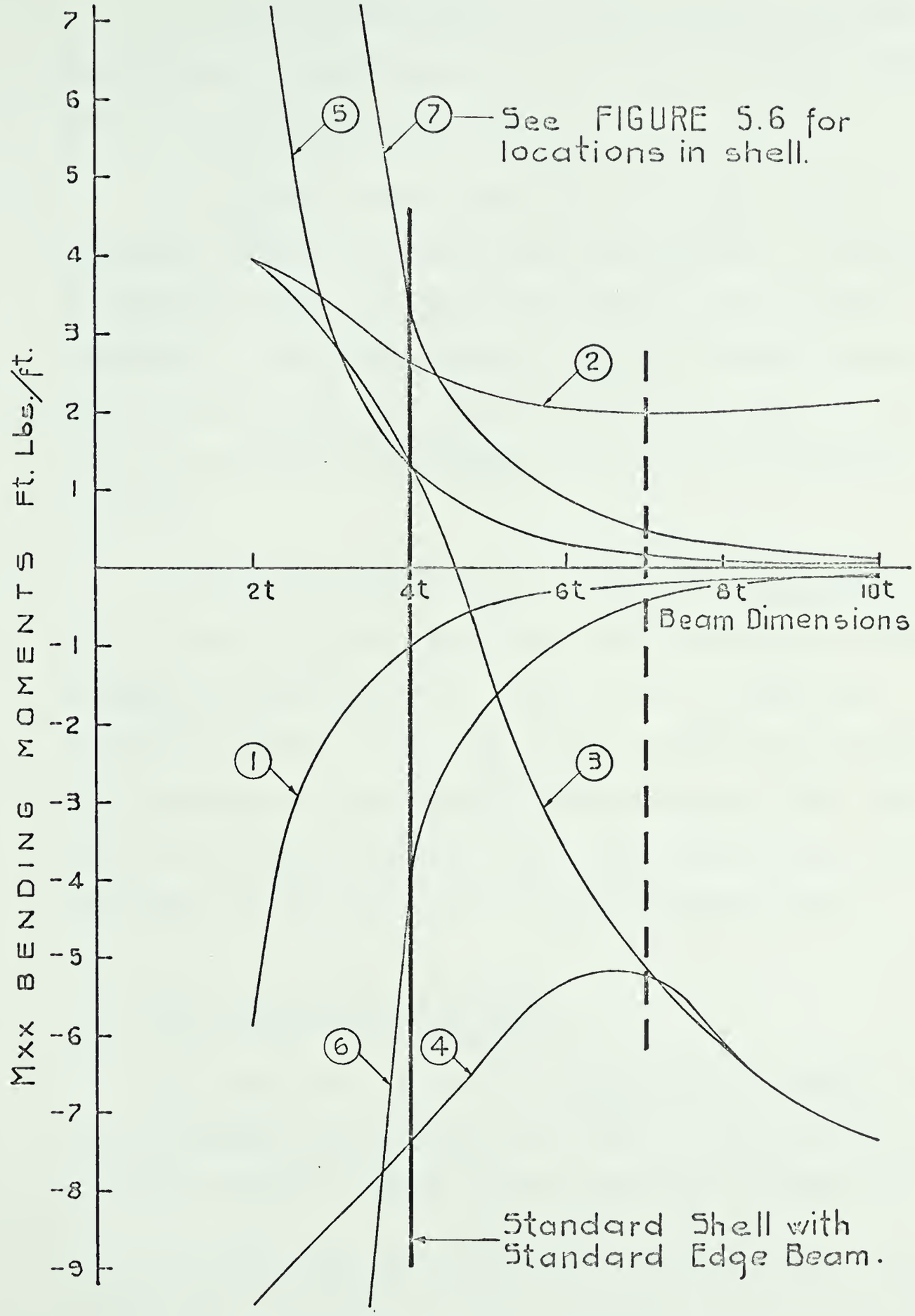

FIGURE 5.7 BENDING MOMENTS Mxx FOR SHELLS SUPPORTED BY ELASTIC EDGE BEAMS, SIZE OF EDGE BEAM SERIES

It should be noted that for all cases except those having very small edge beams (dimensions of 3t or less) the largest bending moments occur along the edge x = a.

The negative bending moment at the mid-edge x = a is a maximum for the shell with edge beams of approximately 10t dimensions. It would appear that for an edge beam of this size the torsional stiffness K3 is sufficiently large to induce a substantial moment, yet the in-plane bending stiffness K4 is not large enough to overwhelm the other stiffnesses, which happens in the limit, as discussed in CHAPTER IV.

It would also appear that for shells with edge beams of at least 4t dimension, but not much larger, the Mxx stresses are similar in magnitude and distribution to those of Cases P, J and G as presented in CHAPTER IV. For these cases the edge beam has infinite axial stiffness, but the in-plane bending stiffness is zero. When the size of the edge beam becomes very large, the Mxx stress situation approaches that of the shell with built-in boundaries, Case A.

5.4.2 Mxx - Shape of Edge Beam Series

In this series, for which the shape of the rectangular edge beams of constant area was varied, key values of bending moments Mxx are given in TABLE 5.3 and are present graphically in FIGURE 5.8.

For the shells with edge beams of large d:b ratios, that is the edge beams are deep but narrow, the bending moments are generally very small. As the d:b ratio decreases to unity (the "standard shell"

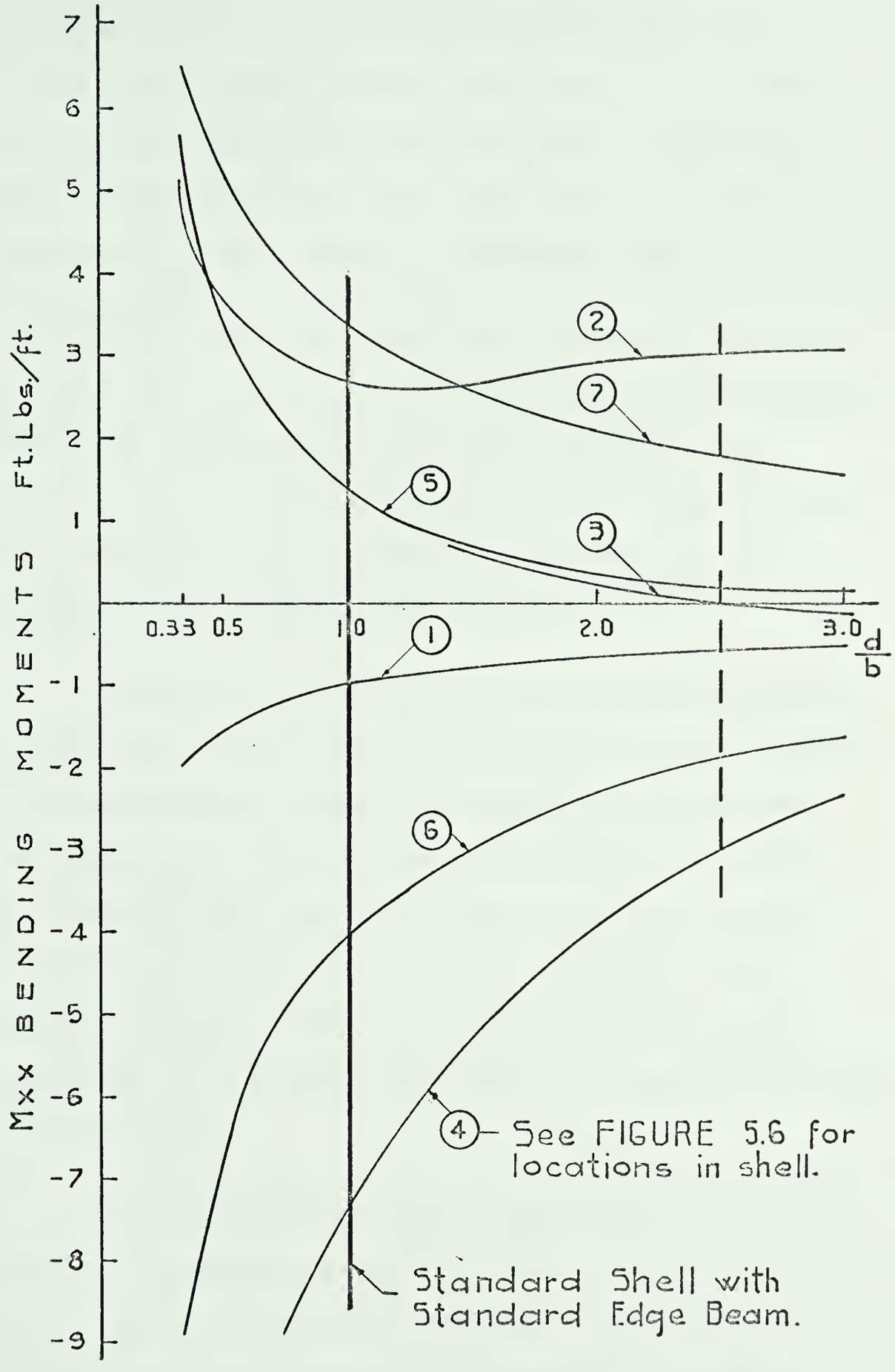

FIGURE 5.8 BENDING MOMENTS Mxx FOR SHELLS SUPPORTED BY ELASTIC EDGE BEAMS, SHAPE OF EDGE BEAM SERIES

with "standard edge beams"), maximum and minimum Mxx values of +2.67 and -7.40 ft.lbs/ft. result. Upon decreasing d:b further, that is the edge beam becomes wide but shallow, bending moments rapidly increase at all locations. Thus this latter configuration of edge beam is highly undesirable from bending moment considerations.

For the shell being considered, there is an optimum d:b edge beam ratio, approximately 2.5, for which the maximum bending moments, both negative and positive, have the lowest value (±3.0 ft.lbs/ft.). This situation is shown by the dashed vertical line in FIGURE 5.8. For d:b decreasing from this value of 2.5, Mxx moments rapidly increase along the edge x = a.

For shells with edge beams in the practical size range the relative flexural stiffness, K4, of the beam is small compared to the corresponding stiffness of the shell and therefore has little effect in preventing in-plane deflections of the shell's edge. In other words, varying the shape of the edge beam does little to vary the effective value of K4. The value of K1 in this series, since the size of the edge beam is kept constant, is not varied. Thus changing the shape of the edge beam effectively varies only K2 and K3.

From TABLE 4.4 it would appear that the most favorable condition for moment occurs when K2 is large and K3 is small, ie Cases F, C and B. As d:b is increased from unity the value of K2 is increased and K3 is decreased, which results in decreasing moments.

5.4.3 Mxx - Variation of Rise to Span Ratio Series

The variable under consideration in this series is the rise h, in terms of h/a, for shells having the "standard edge beam". Bending moments for the same seven key locations considered in sections 5.4.1 and 5.4.2 are given in TABLE 5.3, and are plotted in FIGURE 5.9.

Decreasing the h/a ratio (rise to span ratio) below 0.16 (the "standard shell") results in rapidly increasing positive bending moments along the line y = 0, at a point about 0.2a from the edge. The location of the positive bending moment moves toward the crown as the shell becomes shallower.

Surprisingly, the negative bending moments along the edge x = a near location 4 (see FIGURE 5.9), decrease until the shell approaches the configuration of a plate, at which the moments become very large. This is borne out by the deflection of the shell, which in the vicinity of the corner is upward, and more so for the shells of large h/a ratios. Thus there is a lesser change in the curvature for the shells along the edges, and would appear to explain the smaller moments for the shallower shells.

As shown by the vertical dashed line in FIGURE 5.9, for a ratio of h/a of approximately 0.075, the range of positive and negative bending moments is a minimum. For this case the absolute maximum moment has a value of 5 ft.lbs/ft. The extreme shallowness of the shell for which this occurs is interesting, since for the

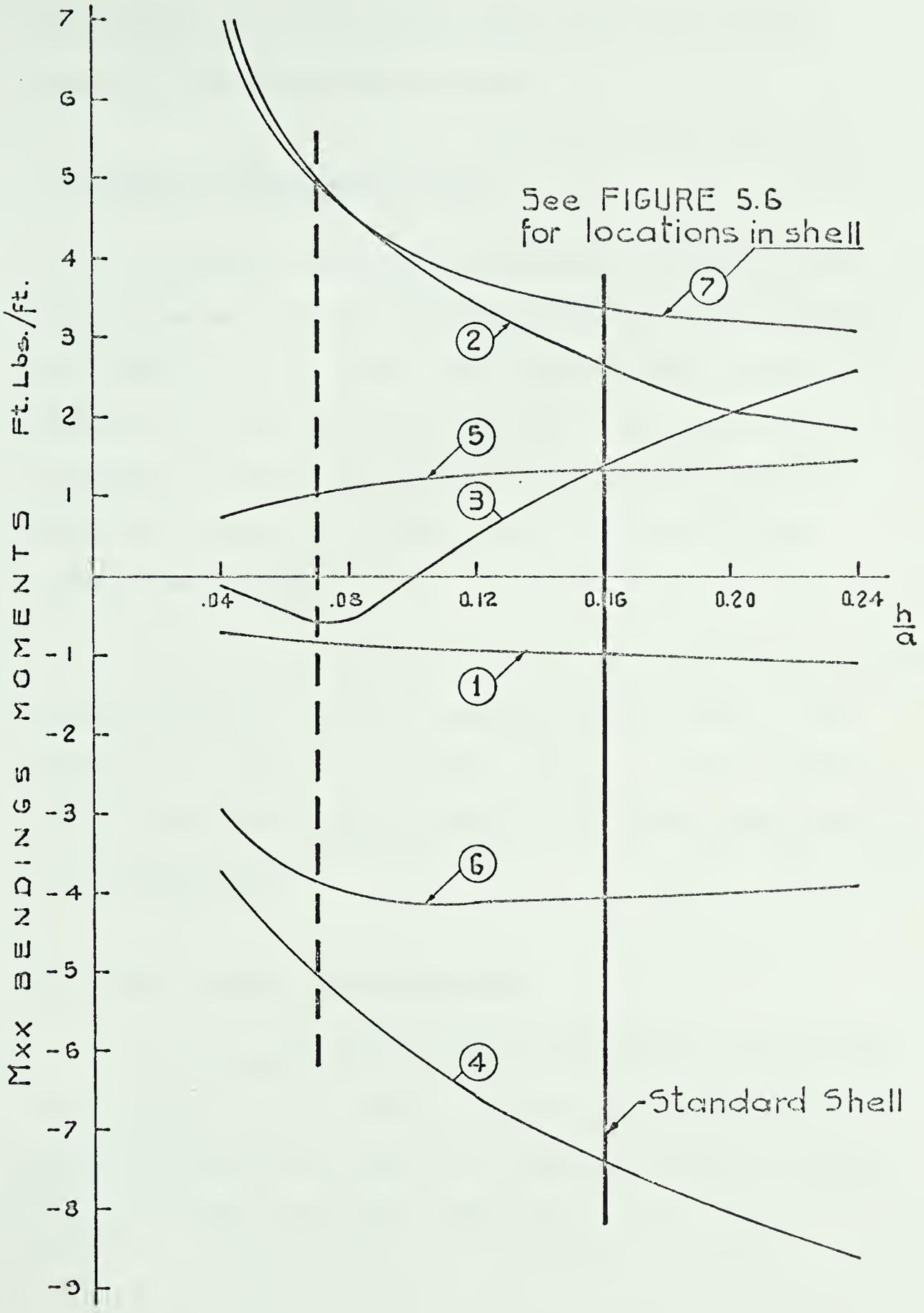

FIGURE 5.9 BENDING MOMENTS Mxx FOR SHELLS SUPPORTED BY ELASTIC EDGE BEAMS, VARIATION OF RISE TO SPAN RATIO SERIES

shells having idealized boundary conditions, shallow shells apparently have larger bending moments.

5.5 Shearing Stress Resultants Nxy

It must be noted, as was discussed in CHAPTER IV, that the location and the values of maximum shearing stress resultants Nxy, which in most cases must occur along the shell's edge at the corner, are not obtained using this model. The reason for this is the method of defining the location of the u and v displacement components at points that are at best one-half grid spacing removed from the edge.

The Nxy stress patterns are similar for all the variations of size or shape of edge beam presented in this chapter. The variations in magnitude are slight, except in the immediate region of the corner support, for all shells having edge beams of practical dimensions.

5.5.1 Nxy - Size of Edge Beam Series

The maximum shearing stress resultants Nxy, which occur in the shell at $x = y = .95a$, for the shell with varying sizes of square edge beams, are presented in FIGURE 5.10, and the maximum calculated values are given in TABLE 5.4.

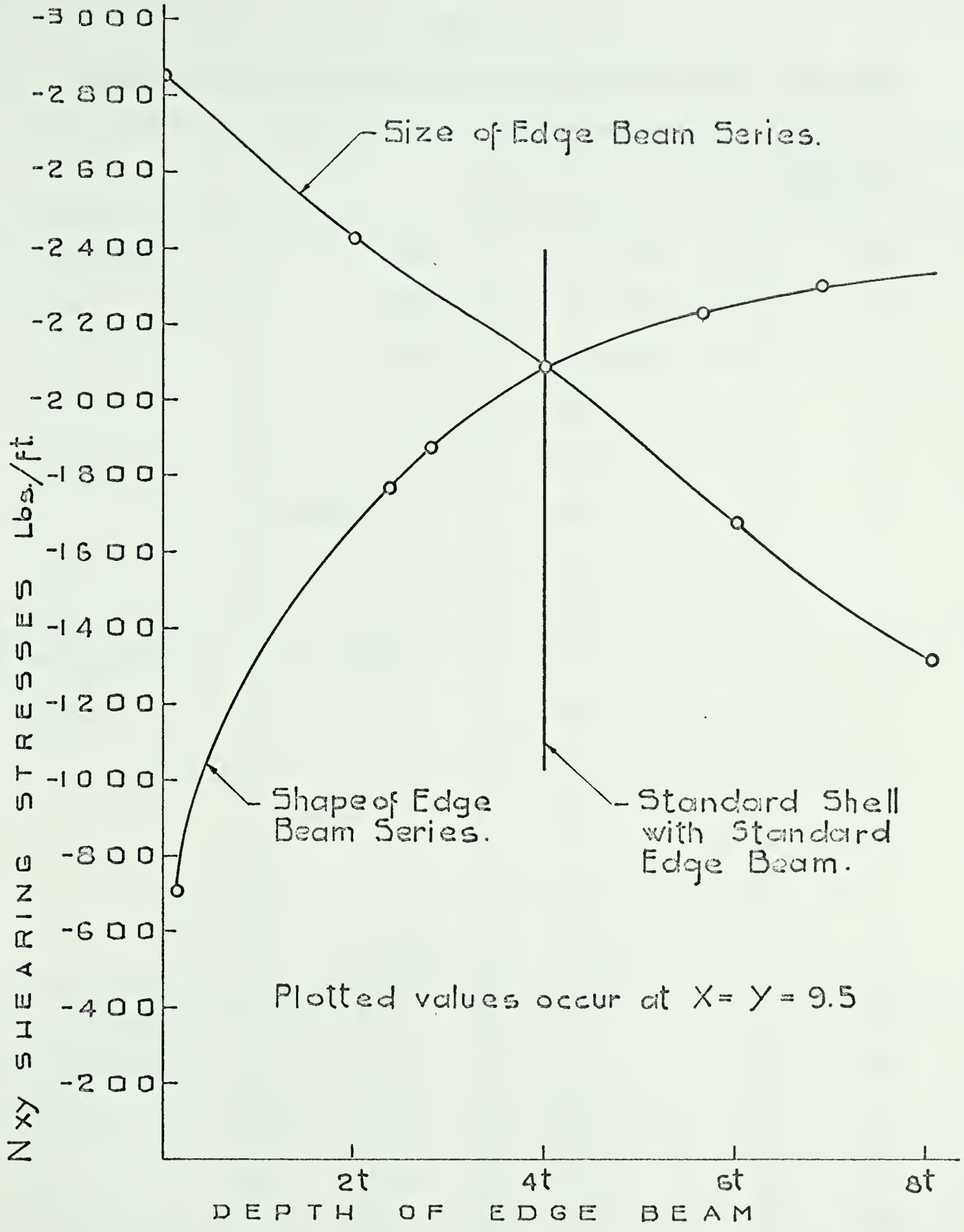

FIGURE 5.10 MAXIMUM SHEARING STRESSES Nxy
FOR SHELLS SUPPORTED BY ELASTIC EDGE BEAMS

TABLE 5.4

SHEARING STRESSES Nxy FOR SHELLS SUPPORTED BY ELASTIC EDGE BEAMS

		Nxy at x=y=0.95a * lbs/ft.	Membrane Theory Nxy at x=a, Y=0.95a lbs/ft
Size of Edge Beam Series	d = b = 1000t	- 148 (Max -155)	-2445
	100t	- 148 (Max -158)	"
	10t	-1070 (Max -1167)	"
	8t	-1324	"
	6t	-1683	"
	Standard 4t	-2097	"
	2t	-2429	"
	0t	-2858	"
Shape of Edge Beam Series	d:b = 1000:1	-2191	-2445
	3:1	-2311	"
	2:1	-2249	"
	Standard 1:1	-2097	"
	1:2	-1894	"
	1:3	-1760	"
	1:1000	- 736	"
Variation of Rise to Span Ratio Series	h/a = 0.24	-1298	-1630
	0.20	-1614	-1955
	Std. 0.16	-2097	-2445
	0.12	-2911	-3250
	0.08	-4531	-4890
	0.04	-9195	-9777

* Nxy at this location is also maximum calculated value, unless noted.

The maximum calculated values of Nxy occur at the secondary grid-point nearest to the corner when d = b = 10t or larger, and occur at the next nearest secondary grid-point when d = b = 8t or less. For the standard shell, the maximum calculated value for Nxy is -2097 lbs./ft.

When the square edge beam has dimensions of less than 10t, for the shell configuration used in this study, the maximum calculated shearing stress decreases linearly with the side dimension of the beam, which indicates the dependence of shearing stresses near the edge on the size of the edge beam. For these cases, in which full fixity of the edge is not approached, there is no significant change in the magnitude of Nxy in the central region of the shell. The "standard shell's" shearing stress pattern is similar to that of a hypothetical case having edge beam stiffness properties between those of Cases J, P, B, N and G, E, Q, L.

By comparing Nxy values in TABLE 5.4 with those in TABLE 4.5, it would appear that the "standard shell's" edge beam has sufficient axial stiffness to make Nxy stresses compare closely in magnitude to those of Cases J, P, B and N. For the "standard shell", the "standard edge beams" cross-sectional area is 1/7th that of half the shell's cross-sectional area, and appears to be sufficient to create a condition close to axial fixity, at least as far as Nxy stresses are concerned.

A comparison was made between the results of the "standard shell" and results obtained using a membrane analysis. This comparison reveals the membrane solution has Nxy magnitudes not exceeding the "standard shell" Nxy magnitudes by more than 20% except within a distance of 0.05a from the corner. At the corner the membrane solution yields mathematically infinite shearing stresses which obviously cannot exist.

5.5.2 Nxy - Shape of Edge Beam Series

The maximum calculated values of the shearing stress resultants Nxy for this series are given in TABLE 5.4 and are plotted in FIGURE 5.10.

In the interior region of the shell the value of Nxy does not vary significantly for those shells having edge beams of practical shape. Within a distance of not more than 0.2a from the corner, the variation in magnitude of Nxy becomes more pronounced. Next to the corner, at $x = y = .95a$, which is also the point where the maximum calculated Nxy stresses occur, the magnitude decreases linearly with an increase in the width of the edge beam. This would appear to indicate the importance of making the edge beam wide in relation to its depth if Nxy stresses in the shell were the only consideration. The shallower but wider edge beam, in allowing greater deflection of the shell's edge, picks up more of the load in the midspans, thus lowering the Nxy stresses at the corner.

5.5.3 Nxy - Variation of Rise to Span Ratio Series

The maximum calculated shearing stresses for this series are presented in TABLE 5.4, and occur at the location x = y = .95a. The shearing stress distributions near the edge of the shell, for all h/a values, are similar to that of the standard shell with the standard edge beam, for which the Nxy stresses are presented in FIGURE 4.5.

Variation of the h/a ratio is actually a variation of the curvature of the shell, commonly described by the curvature factor, a^2/h. A study of the maximum calculated Nxy values indicates a linear relationship between Nxy and the curvature factor. The membrane solution also yields a similar linear relationship.

Thus, decrease in curvature results in increasing shearing stresses.

5.6 Summary

In this chapter, the stiffness parameters were evaluated for shells having elastic edge beams. The effects on the shell, but not the effects on the edge beams, have been discussed.

Over their total range of values, the stiffness parameters have a complex interacting effect. However, within the normal range of values, the following practical conclusions can be made.

The in-plane bending stiffness K4 is effectively zero, as the in-plane stiffness of the shell overwhelms that of the edge beam. The torsional stiffness K3 is also relatively insignificant in its effect on the shell, even in the immediate vicinity of the edge where its greatest influence exists.

The axial stiffness K1 and the transverse bending stiffness K2 have significant effect on the behaviour of the shell, in the limit as well as in the practical range of values. In preventing in-plane shearing deformations at the edge, K1 has the greatest effect, and by preventing normal deflections along the edge, K2 has a lesser but also significant effect.

It would appear desirable, from deflection and stress considerations, to make the edge beam of elliptic paraboloid shells as large as possible, and to make the beam deep compared to its width. The shallower the shell, the more severe generally are the stress effects on the shell.

CHAPTER VI

SUMMARY AND CONCLUSION

The behaviour of elliptic paraboloid shells under uniform normal loading with idealized boundary conditions is significantly different from the behaviour exhibited by shells with elastic edge beams of practical dimensions.

When in-plane outward movement of the shell's edge is prohibited (K4 = infinity), the load is carried solely by membrane action, that is arching to the edge, with little or no bending for uniformly distributed loads. This condition cannot be realized in practical situations except for continuous shells.

It is significant which mechanism, either tangential shear stresses or transverse edge forces, is acting in preventing normal movement of the shell's edge. In the former case, the axial stiffness K1 is large and there is relatively little bending in the shell, whereas in the latter case, significant bending stresses are induced by the transverse forces developed by the large bending stiffness K2. Thus it is not sufficient to know that the edge of the shell is prevented from deflecting, one must know how the edge of the shell is prevented from deflecting.

Practical shells can be considered unrestrained in outward in-plane movement at the edge, but generally the edge beam has sufficient area to be considered stiff, relative to the shell, in the axial direction. Thus the load is carried predominantly by membrane

action. Practical edge beams are also usually stiff enough to carry part of the load by beam action, in which case significant bending stresses result in the shell, caused by the transverse forces at the edge.

The torsional stiffness K3 of the elastic edge beams is generally not significant in its effect, especially when in-plane direct or shear forces exist at the boundary. In practical situations it could probably be ignored.

Edge beams that are deep compared to their width result in more favorable stress conditions. It is also important that the edge beams have sufficient cross-sectional area to create a membrane stress condition in the shell. Edge beams designed as arches, with dimensions based on the tangential shear forces arrived at by the membrane analysis, would appear to be near the lower size limit if stresses in the shell are to be kept low.

LIST OF REFERENCES

LIST OF REFERENCES

1. Abu-Sitta, S. H. - "Finite difference solutions of the bending theory of the elliptic paraboloid". Bulletin of the International Association for Shell Structures, December, 1964.

2. Marguerre, K. - "Zur Theorie der gekrummten Platte grosser Formaderung" 5th International Congress on Applied Mechanics, 1938.

3. Noor, A. K. - "Analysis of doubly curved shallow shells". Ph. D. Thesis, University of Illinois, 1963.

4. Parme, A. L. - "Hyperbolic paraboloids and other shells of double curvature". Journal of the Structural Division, ASCE, Vol. 82, No. ST. 5, September, 1956.

5. Rajendram, I. - "Method of analysis of shallow translational shells". M. Sc. Thesis, University of Alberta, 1965.

6. Padilla, J. C. and Schnobrick, W. C. - "Analysis of shallow doubly-curved shells supported by elastic edge members". Structural Research Series No. 310, University of Illinois, June, 1966.

7. Simmonds, S. H. - Discussion, proceedings of the International Symposium on Shell Structures in Engineering Practice, Budapest, Hungary, September, 1965.

8. Timoshenko, S. and Woinowsky-Krieger, S. - "Theory of Plates and Shells". McGraw Hill, 1940.

9. Vlassov, V. Z. - Basic differential equations in general theory of elastic shells". Prikladnaya Matematica i Mechanika, Vol. 8, 1944 (in Russian) Translated into English in NACA TM-1241, February, 1951.

10. White, R. N. - "Optimum solution techniques for finite difference equations" ASCE Proc. V89 (J. Str. Div.) St. 4, August, 1963, Part 1.